Bioorganic & Medicinal Chemistry 18 (2010) 5352–5366

Contents lists available at ScienceDirect

Bioorganic & Medicinal Chemistry

journal homepage: www.elsevier.com/locate/bmc

Design, synthesis, and biological evaluation of resveratrol analogues as aromatase and quinone reductase 2 inhibitors for chemoprevention of cancer

Bin Sun [a,†], Juma Hoshino [a], Katie Jermihov [c], Laura Marler [b], John M. Pezzuto [b], Andrew D. Mesecar [c], Mark Cushman [a,*]

[a] Department of Medicinal Chemistry and Molecular Pharmacology, School of Pharmacy and Pharmaceutical Sciences, and The Purdue Center for Cancer Research, Purdue University, West Lafayette, IN 47907, United States
[b] College of Pharmacy, University of Hawaii at Hilo, Hilo, HI 96720, United States
[c] Center for Pharmaceutical Biotechnology and Department of Medicinal Chemistry and Pharmacognosy, College of Pharmacy, The University of Illinois at Chicago, Chicago, IL 60612, United States

ARTICLE INFO

Article history:
Received 5 March 2010
Revised 11 May 2010
Accepted 14 May 2010
Available online 24 May 2010

Keywords:
Resveratrol analogues
Aromatase
Quinone reductase 2

ABSTRACT

A series of new resveratrol analogues were designed and synthesized and their inhibitory activities against aromatase were evaluated. The crystal structure of human aromatase (PDB 3eqm) was used to rationalize the mechanism of action of the aromatase inhibitor **32** (IC_{50} 0.59 μM) through docking, molecular mechanics energy minimization, and computer graphics molecular modeling, and the information was utilized to design several very potent inhibitors, including compounds **82** (IC_{50} 70 nM) and **84** (IC_{50} 36 nM). The aromatase inhibitory activities of these compounds are much more potent than that for the lead compound resveratrol, which has an IC_{50} of 80 μM. In addition to aromatase inhibitory activity, compounds **32** and **44** also displayed potent QR2 inhibitory activity (IC_{50} 1.7 μM and 0.27 μM, respectively) and the high-resolution X-ray structures of QR2 in complex with these two compounds provide insight into their mechanism of QR2 inhibition. The aromatase and quinone reductase inhibitors resulting from these studies have potential value in the treatment and prevention of cancer.

1. Introduction

Resveratrol (3,5,4′-trihydroxystilbene) (Fig. 1) was first isolated from the roots of the white hellebore lily *Veratrum grandiflorum* O. Loes in 1940.[1] This compound is a naturally occurring phytoalexin produced by a wide range of plants (at least 72 plant species) in response to environmental stress or pathogenic attack. Since the discovery of its cardioprotective activity in 1992, resveratrol research has steadily accelerated. This increased attention eventually resulted in the discovery of its cancer chemopreventive properties.[2] Resveratrol was found to be capable of interfering with all three steps of carcinogenesis (initiation, promotion, and progression).[2]

Resveratrol has been reported to exert a variety of biological activities. Some of these include antioxidant, anti-inflammatory, anti-infective, anti-ischemic, cardioprotective, neuroprotective, anti-aging (prolongs lifespan), anti-obesity, anti-viral, and cancer chemopreventive effects.[3] These effects are mediated through several biological receptors, including cyclooxygenase (COX), lipooxygenase (LOX), nuclear factor kappa-light-chain-enhancer of activated B cells (NF-kB), quinone reductase 1 (QR1), quinone reductase 2 (QR2), ornithine decarboxylase (ODC), and aromatase.

In the United States, breast cancer is the most commonly diagnosed type of cancer in women and is the second leading cause of death from cancer in women. Approximately 180,000 new cases of breast cancer were detected among women in the United States in 2008.[4] About two-thirds premenopausal and three-fourths postmenopausal breast cancer patients have estrogen-dependent cancer.[5]

In hormone-dependent breast cancer, estrogens play a critical role in stimulating breast cancer cell proliferation.[6] High levels of estrogens promote the progression of breast cancer. Two main strategies have been devised by medicinal chemists to control or block the pathological activity of estrogens.[7] The first strategy involves

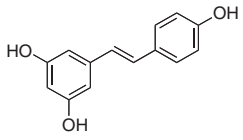

Resveratrol
IC_{50} 80 μM (Aromatase)

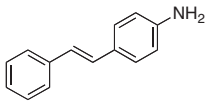

JH-2-29
IC_{50} 22 μM (Aromatase)

Figure 1. Chemical structures of resveratrol and compound **JH-2-29**.

* Corresponding author. Tel.: +1 765 494 1465; fax: +1 765 494 6790.
E-mail addresses: cushman@purdue.edu, cushman@pharmacy.purdue.edu (M. Cushman).
† On leave from Shandong University, China.

0968-0896/$ - see front matter © 2010 Elsevier Ltd. All rights reserved.
doi:10.1016/j.bmc.2010.05.042

the design and synthesis of estrogen receptor antagonists, which has yielded useful anticancer and chemopreventive drugs such as tamoxifen and raloxifene.[8,9] Aromatase, a pivotal enzyme responsible for the conversion of androgens to estrogens, is 'the other' attractive biological target for the development of new agents for the treatment of breast cancer.[10–14] As the enzyme responsible for the final step of the estrogen biosynthetic pathway, selective inhibition of aromatase will not interfere with the production of other steroids in the pathway (e.g., adrenal corticoids).[15,16] Therefore, aromatase is a useful therapeutic target in the treatment or prevention of estrogen-dependent breast cancers.[17]

Quinone reductase 2 (QR2) is a cytosolic FAD-dependent flavoenzyme that catalyzes the reduction of quinones by reduced *N*-alkyl- and *N*-ribosylnicotinamides.[18] Recent studies have indicated that QR2 may transform certain quinone substrates into more highly reactive species that are capable of causing increased cellular damage.[19–21] Therefore, it is hypothesized that inhibition of QR2 in certain cases may lead to protection of cells against these reactive species.[18] Several QR2 inhibitors have been reported in the literature[22] and the X-ray crystal structure of QR2 in complex with resveratrol has been determined.[23,24] These observations motivated the present study.

Both aromatase and QR2 have been targeted for discovery and identification of chemopreventive agents.[24] An array of resveratrol analogues have been synthesized in our laboratory in an attempt to discover new inhibitors of these two enzymes. The *trans*-stilbene **JH-2-29** (Fig. 1, Scheme 7), with a *para*-amino group, was found to exhibit versatile biological activities including nitric oxide synthase inhibition, aromatase inhibition (IC_{50} 22 μM), and inhibition of TNF-α-induced NF-κB activity, and was therefore selected as a lead compound for further optimization. In order to improve the potency and selectivity of **JH-2-29**, a limited number of methoxylated compounds were synthesized and observed empirically to enhance aromatase inhibitory activity. In particular, compound **32** (Fig. 2) was found to possess significant aromatase inhibitory activity, with an IC_{50} value of 0.59 μM, which is comparable to the clinically useful aromatase inhibitor 2-aminoglutethimide (IC_{50} 0.27 μM) (Fig. 2).[18] Molecular modeling was used to investigate the mechanism of action, and a variety of structurally related stilbenes were designed and synthesized based on the results. Several of these synthetic derivatives were found to inhibit aromatase activity with IC_{50} values in the sub-micromolar range. In addition, two compounds, **32** and **44**, were discovered to exhibit potent QR2 inhibitory activity, and X-ray crystallographic analysis revealed these two compounds bind to QR2 in an orientation similar to that of resveratrol, but both compounds demonstrate greater inhibitory potency than resveratrol.

2. Results and discussion

2.1. Chemistry

Preparation of the *trans*-stilbene derivatives **32**–**59** was accomplished mainly by means of the Wittig reaction between the appropriately substituted aromatic aldehydes **1–12** and methyl triphenylphosphonium bromide, and the following Heck reaction between appropriately substituted vinylbenzenes **11**–**22** and iodobenzenes **23**–**31** as shown in Scheme 1 and Table 1. The coupling constants of the vinylic protons of the *trans*-stilbenes were about 16 Hz. The double bonds of the analogues **32**, **37**, **41**, and **49** were reduced by catalytic hydrogenation to provide the corresponding derivatives **60**, **61**, **62**, and **63** (Scheme 2). Dinitro analogues **50** and **52** were reduced with stannous chloride to provide the respective polyamines **64** and **65** in satisfactory yields (Scheme 3). The acetate groups of compounds **39** and **55** were hydrolyzed by sodium methoxide in methanol to yield phenol derivatives **66** and **67** (Scheme 4). The *tert*-butyldimethylsilyl (TBDMS)-protected vinylbenzene **69** (Scheme 5) reacted with 4-iodoaniline in a standard Heck reaction, but the yield was very low. The method of Angela et al. was used and the TBDMS group of intermediate compound **69** was cleaved by tetrabutylammonium fluoride (TBAF) to afford the diphenol **70**, which was acetylated to produce **71**. Heck reaction between compound **71** and 4-iodoaniline or 4-iodonitrobenzene led to the respective *trans*-stilbenes **72** and **73**. Acetate hydrolysis yielded the desired compounds **74** and **75**.[25] The synthetic route to imidazole analogue **82** began with the preparation of phosphonium salt **78** from aldehyde **5**, and ketone **80** from commercially available compound **79** (Scheme 6). The building blocks **78** and **80** were then combined by the Wittig reaction in the presence of potassium carbonate and 18-crown-6,[26,27] and the resulting *E* and *Z* isomers were separated and purified by chromatography to provide the nitro analogue **82**. Reduction by stannous chloride resulted in the amine derivative **84** (Scheme 6). The double bond conformation of compound **82** was confirmed by 2D ^{1}H–1H NOESY spectroscopy (Fig. 3).

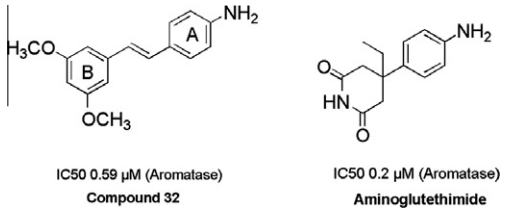

Figure 2. Chemical structures of compound **32** and aminoglutethimide.

2.2. Mechanism

The aromatase inhibitory activity of the resveratrol analogue **32** (IC_{50} 0.59 μM) in comparison with resveratrol itself (IC_{50} 80 μM) led to an investigation of the mechanism of action of compound **32**. Recently, Ghosh et al. solved the crystal structure of human aromatase in complex with androgen.[28] Compound **32** was docked into the binding site of Ghosh's structure (PDB code 3eqm) using the GOLD (Genetic Optimization for Ligand Docking) program,[29–31] and the energy minimized. In the resulting hypothetical structure (Fig. 4), the amine group on ring A hydrogen bonds with the carbonyl group of Ile305 and carboxyl group of Asp309, which plays a critical role in catalysis.[28] Ring A is involved in a π–π interaction with the indole ring of Trp224, and a CH–π interaction with the methyl group of Thr310. Ring B forms a CH–π interaction with the methyl group of Val370. The methoxyl group on ring B is involved in a potential hydrogen bond with the backbone NH of Met374. All of the residues mentioned above are included in the catalytic cleft of aromatase.[28]

The docking and energy minimization results provide a good foundation for design of new analogues. In order to minimize the possible cytotoxicity contributed by the aniline part of compound **32**, the amino group on ring A was replaced by hydrogen bond-donating groups, such as hydroxy and aminomethyl groups, which may form hydrogen bonds with Asp309 and Ile305 (Fig. 5). As shown in Figure 4, the backbone carbonyl group of residue Leu477, a potential hydrogen bond acceptor located near ring B, suggested the addition of hydrogen bond-donating groups on ring B. Met374, working as a hydrogen bond donor, also suggests incorporation of hydrogen bond acceptors on ring B. In order to probe the function of the stilbene double bond, compounds with single bonds were also synthesized. Many aromatase inhibitors have imidazole or triazole groups that can coordinate to the iron atom,[32–36] and these were therefore added to the stilbene framework and the resulting structures were modeled in complex with aromatase.

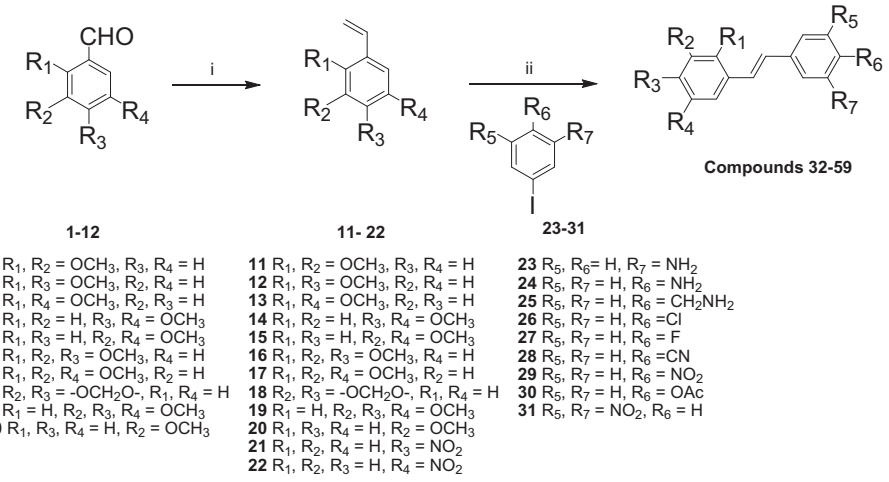

Scheme 1. Reagents and conditions: (i) CH_3PPh_3Br, $NaNH_2$, Et_2O, rt; (ii) KOAc, $Pd(OAc)_2$, Bu_4NBr, DMF, 50–80 °C.

Table 1
Structures of compounds **32**–**59**

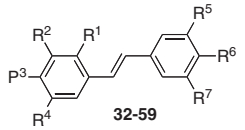

Compd	R_1	R_2	R_3	R_4	R_5	R_6	R_7
32	H	OCH_3	H	OCH_3	H	NH_2	H
33	OCH_3	H	OCH_3	H	H	NH_2	H
34	OCH_3	H	OCH_3	H	NH_2	H	H
35	OCH_3	H	H	OCH_3	H	NH_2	H
36	OCH_3	OCH_3	H	H	H	NH_2	H
37	H	OCH_3	OCH_3	H	H	NH_2	H
38	H	OCH_3	OCH_3	H	H	CN	H
39	H	OCH_3	OCH_3	H	H	OAc	H
40	H	OCH_3	OCH_3	H	H	F	H
41	H	OCH_3	OCH_3	OCH_3	H	NO_2	H
42	H	OCH_3	OCH_3	OCH_3	NH_2	H	H
43	H	OCH_3	OCH_3	OCH_3	H	CH_2NH_2	H
44	H	OCH_3	OCH_3	OCH_3	H	NH_2	H
45	OCH_3	OCH_3	OCH_3	H	H	NH_2	H
46	OCH_3	OCH_3	H	OCH_3	H	NH_2	H
47	H	$-OCH_2O-$		H	NH_2	H	H
48	H	$-OCH_2O-$		H	H	NH_2	H
49	H	H	NO_2	H	NO_2	H	H
50	H	NO_2	H	H	H	NH_2	H
51	H	OCH_3	H	H	H	NH_2	H
52	H	H	NO_2	H	NO_2	H	NO_2
53	H	OCH_3	H	OCH_3	H	NO_2	H
54	H	OCH_3	H	OCH_3	NH_2	H	H
55	H	OCH_3	H	OCH_3	H	OAc	H
56	H	OCH_3	H	OCH_3	H	CH_2NH_2	H
57	H	OCH_3	H	OCH_3	H	F	H
58	H	OCH_3	H	OCH_3	H	Cl	H
59	H	OCH_3	H	OCH_3	H	CN	H

2.3. Aromatase inhibitory activity

An aromatase inhibition assay was performed on synthetic analogues of compound **JH-2-29**, as described in the Section 4. The inhibition percentage at a concentration of 20 μg/mL and the IC_{50} values of the more active compounds are reported in Table 2. Most of the resveratrol analogues with an amino group on the para position of ring A (**32**, **33**, **35**, **36**, **37**, **44**, **45**, **46**, **48**, **51**, **64**, **65**, **72**, and **74**) consistently exhibited significant activity, with IC_{50} values in the 0.59–14.51 μM range. Substitution of the *para*-amino group with nitro, halogen, hydroxy, nitrile, acetyl, and aminomethyl groups made the resulting compounds inactive (compounds **38**, **39**, **40**, **41**, **43**, **52**, **53**, **55**, **56**, **57**, **58**, **59**, **66**, **67**, and **75**). Changing the position of amino group on ring A also led to reduced activity (compounds **34**, **42**, and **54**). Presumably, altering the position of the amino group is expected to influence its ability to simultaneously hydrogen bond with the Asp309 carboxylate and the backbone carbonyl oxygen of Ile305 (Fig. 4). Double bond reduction impacted the activity positively (**37** vs **61**, **49** vs **63**, and **41** vs **62**) or negatively (**32** vs **60**) to some extent. Within the series, the position of amino group on ring A was of greater importance than that of methoxy groups (ring B), and a *para*-amino group was better than an *ortho*- or *meta*-amino group.

Compound **84** was the most potent aromatase inhibitor, with an IC_{50} value of 36 nM. As expected, molecular modeling indicated that one of the imidazole nitrogens coordinates with the iron atom of heme, which plays a critical role in catalysis (Fig. 6).[28]

K_M and V_{max} values for those analogues demonstrated to inhibit aromatase can be found in Table 3. V_{max} values for each inhibitor are quite similar to each other and to the V_{max} of the control (34.8 pmol/min/mg protein), indicating that these resveratrol analogues are competitive inhibitors of CYP19.

2.4. Quinone reductase 2 inhibitory activity and X-ray structure analysis

QR2 inhibition assays were performed on analogues of synthetic compound **JH-2-29**, as described in the Section 4. Compounds **32** and **44** exhibited potent QR2 inhibitory activity with IC_{50} values of 1.7 ± 0.06 μM and 0.27 ± 0.01 μM, respectively. Both of these substances are more potent than resveratrol, which has an IC_{50} value of 5.1 μM in the same assay.

To gain insight into the binding mode of these two inhibitors, the X-ray crystal structures of both compounds **32** and **44** in complex with human QR2 were determined. Complete X-ray data sets were collected and processed, and the final structural models were refined to 1.74 Å and 1.55 Å for compound **32** and compound **44** complexes, respectively. As revealed by the strong and well-defined electron density shown in Figure 7, both compounds **32** and **44** bind to QR2 in an orientation similar to that of resveratrol. However, these two compounds interact directly with the side chain of Thr71, whereas resveratrol binds to this residue indirectly through a water molecule. The direct hydrogen bond interaction between the amino group and the hydroxyl group of residue Thr71 is most likely responsible for enhancing the QR2 inhibitory activity of compounds **32** and **44** relative to resveratrol. The 3-

32 R_1, R_3 = OCH_3, R_2 = H, R_4 = NH_2
37 R_1, R_2 = OCH_3, R_4 = NH_2
41 R_1, R_2, R_3 = OCH_3, R_4 = NH_2
49 R_1, R_4 = NO_2, R_2, R_3 = H

60 R_1, R_3 = OCH_3, R_2 = H, R_4 = NH_2
61 R_1, R_2 = OCH_3, R_4 = NH_2
62 R_1, R_2, R_3 = OCH_3, R_4 = NH_2
63 R_1, R_4 = NH_2, R_2, R_3 = H

Scheme 2. Reagents and conditions: (i) H_2, Pd/C, MeOH.

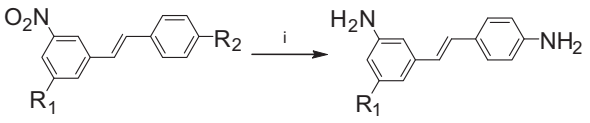

50 R_1 = H, R_2 = NH_2
52 R_1 = NO_2, R_2 = NO_2

64 R_1 = H
65 R_1 = NH_2

Scheme 3. Reagents and conditions: (i) $SnCl_2$, EtOH.

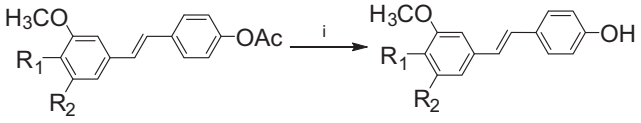

39 R_1 = OCH_3, R_2 = H
55 R_2 = OCH_3, R_1 = H

66 R_1 = OCH_3, R_2 = H
67 R_2 = OCH_3, R_1 = H

Scheme 4. Reagents and conditions: (i) NaOMe, MeOH.

methoxy groups on ring B of compounds **32** and **44** interact with the amide NH_2 group of residue Asn161, and there is one more hydrogen bond interaction between this side chain and the 4-methoxy group of compound **44**, which may contribute to the higher potency of compound **44** relative to **32**. The X-ray structures of QR2 in complex with compounds **32** and **44** also indicate that these resveratrol analogues sit parallel to the plane of the isoalloxazine ring of the bound cofactor FAD, occupying a position that is similar to resveratrol in the QR2-resveratrol complex.[22]

3. Conclusions

A focused set of 45 resveratrol analogues have been designed, synthesized, and tested in an effort to maximize their aromatase and QR2 inhibitory activities. Compounds **82** and **84** exhibit excellent aromatase inhibitory activity, with IC_{50} values 70 nM and 36 nM, respectively. From the preliminary structure–activity relationships and molecular modeling results, it appears that the *para*-amino group on the *trans*-stilbene benzene ring is essential for aromatase inhibitory activity, and the introduction of an imidazole moiety improves the activity greatly. Compounds **32** and **44** also displayed potent QR2 inhibitory activity, and their crystal structures in complex with QR2 have been determined. They provide a detailed description of the enzyme active site, and can be utilized in the further modification for discovery of new QR2 inhibitors.

4. Experimental

4.1. General procedures

Melting points were determined in capillary tubes using a Mel-Temp apparatus and are not corrected. Infrared spectra were obtained as films on salt plates using $CHCl_3$ as the solvent except where otherwise specified, using a Perkin–Elmer Spectrum One FT-IR spectrometer, and are baseline-corrected. ^1H NMR spectra were obtained at 300 MHz (^1H) and 75 MHz (^{13}C) or 500 MHz (^1H) and 125 MHz (^{13}C), using Bruker ARX300 and Bruker Avance 500 (TXI 5 mm probe) spectrometers, respectively. Mass spectral analyses were performed at the Purdue University Campus-Wide Mass Spectrometry Center. Analytical thin-layer chromatography was performed on Baker-flex silica gel IB2-F plastic-backed TLC plates. Flash chromatography was performed with 230–400 mesh silica gel. Unless otherwise stated, chemicals and solvents were of reagent grade and used as obtained from commercial sources without further purification. Dichloromethane was distilled from CaH_2 and THF from sodium prior to use.

4.1.1. General procedure 1 (GP 1) for the preparation of aromatic alkenes from aromatic aldehydes

Methyl triphenylphosphonium bromide (4.3 g, 12.05 mmol) and sodium amide (0.47 g, 12.05 mmol) in dry diethyl ether

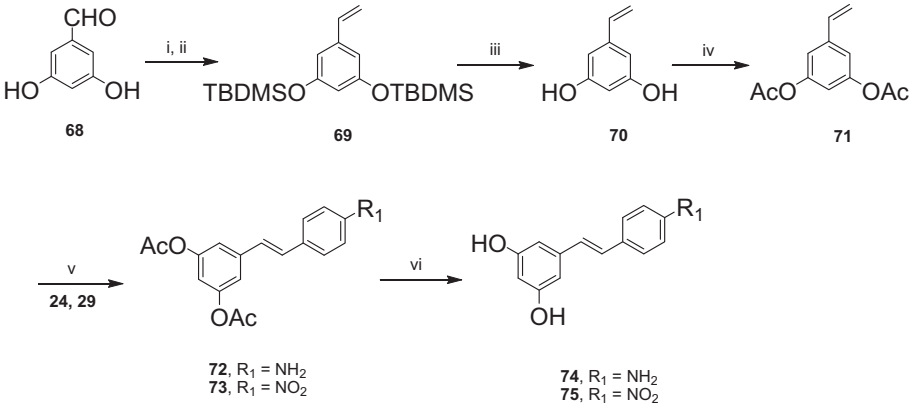

68
69
70
71

72, R_1 = NH_2
73, R_1 = NO_2

74, R_1 = NH_2
75, R_1 = NO_2

Scheme 5. Reagents and conditions: (i) TBDMSCl, DIPEA, DMF; (ii) CH_3PPh_3Br, $NaNH_2$, Et_2O; (iii) TBAF, THF; (iv) Ac_2O, DMAP, DCM; (v) KOAc, $Pd(OAc)_2$, Bu_4NBr, DMF, 70 °C, 10 h; (vi) NaOMe, MeOH.

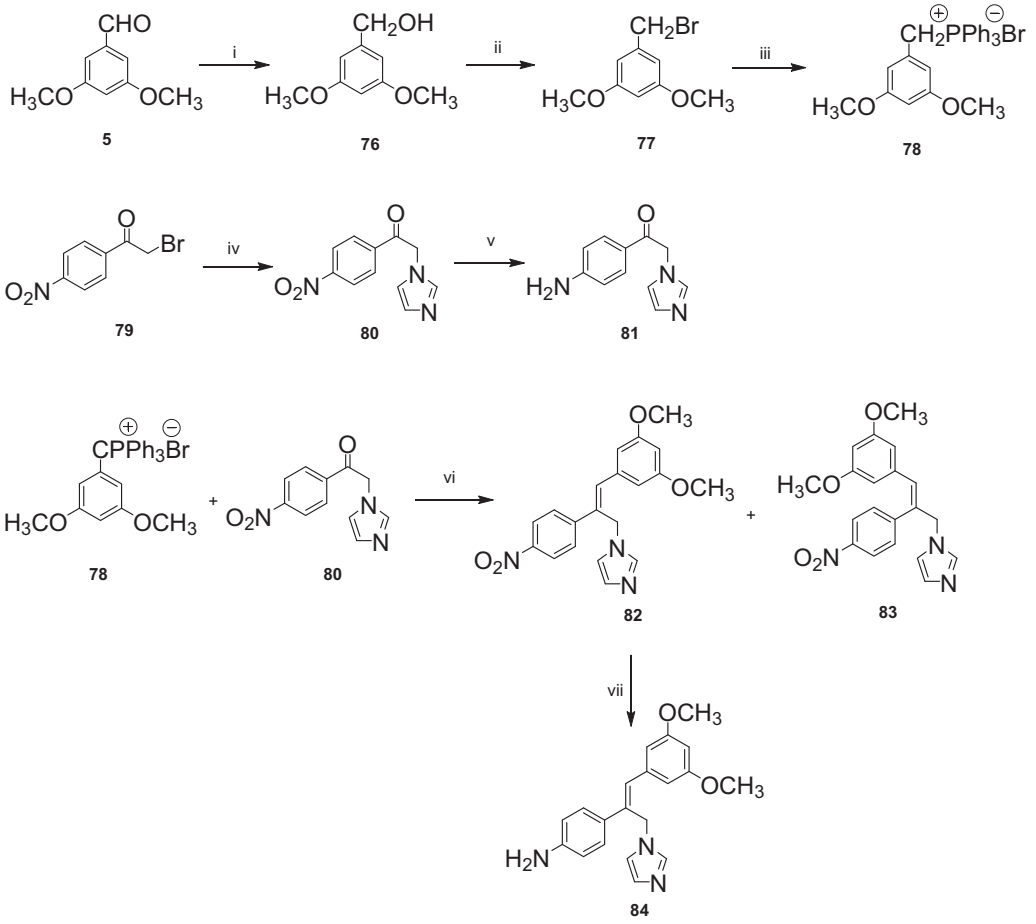

Scheme 6. Reagents and conditions: (i) $NaBH_4$, THF; (ii) PBr_3, DCM; (iii) PPh_3, toluene, reflux; (iv) imidazole, THF, rt; (v) H_2, Pd/C, MeOH; (vi) K_2CO_3, 18-crown-6, DCM, reflux; (vii) $SnCl_2$, EtOH, reflux.

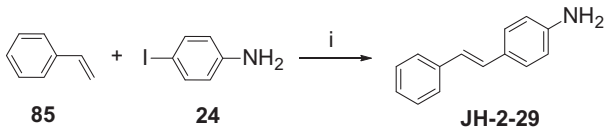

Scheme 7. Reagents and conditions: (i) K_2CO_3, $Pd(OAc)_2$, Bu_4NBr, DMF, 80 °C.

(15 mL) were stirred at room temperature under argon for 10 h. A solution of benzaldehyde (6 mmol) in diethyl ether (10 mL) was added to the reaction mixture dropwise under argon in 30 min at −10 °C. After 10 min, the reaction mixture was warmed up to room temperature and stirred for 2 h. The reaction mixture was then filtered and the solvent was removed in vacuo to yield yellow oil that was purified by silica gel column chromatography, eluting with hexane–dichloromethane mixture, to yield the pure product in good yield.

4.1.2. General procedure 2 (GP 2) for the Heck reactions

In a round-bottomed flask, iodobenzene (2.21 mmol) was added to a mixture of tetrabutylammonium bromide (1.1 g, 3.33 mmol), potassium acetate (350 mg, 3.57 mmol), palladium acetate (25 mg, 0.11 mmol) and aromatic alkenes (2.44 mmol) stirred in DMF (20 mL) at room temperature under argon. The reaction mixture was warmed up to 80 °C for 3 h and then cooled to room temperature. Diethyl ether (25 mL) was added and the organic layer was washed with water (3 × 20 mL) and then dried over anhydrous sodium sulfate. The solution was concentrated and the residue was purified by silica gel column chromatography, eluting with hexane–dichloromethane mixture, to yield the pure product as a solid in moderate yield.

4.1.3. General procedure 3 (GP 3) for the hydrolysis of acetyl groups

NaOMe (2 mg, 0.04 mmol) was added to a solution of (*E*)-(styryl)phenyl acetate (0.5 mmol) in ethanol (15 mL). The reaction mixture was stirred for 10 h and the solvent was evaporated in vacuo. The residue was purified by silica gel column chromatography, eluting with a solution of 1% methanol in dichloromethane, to yield the pure product in good yield.

4.1.4. General procedure 4 (GP 4) for the catalytic hydrogenation of nitro groups and stilbenes

Stilbene compound (0.35 mmol) was dissolved in ethyl acetate (15 mL) and stirred with palladium on carbon (10%, 10 mg) under H_2 at room temperature for 24 h. The mixture was filtered, and the solvent was removed in vacuo to provide a solid that was recrystallized from dichloromethane and hexane to yield the pure product in good yield.

4.2. Syntheses

4.2.1. 1,2-Dimethoxy-3-vinylbenzene (11)[37]

This compound was prepared in 97% yield by following GP 1. Colorless oil. ^1H NMR (300 MHz, $CDCl_3$) δ 7.14–6.99 (m, 3H), 6.82 (dd, J = 10.8 Hz, J = 1.2 Hz, 1H), 5.77 (d, J = 17.7 Hz, 1H), 5.30 (d, J = 11.1 Hz, 1H), 3.84 (s, 3H), 3.81 (s, 3H).

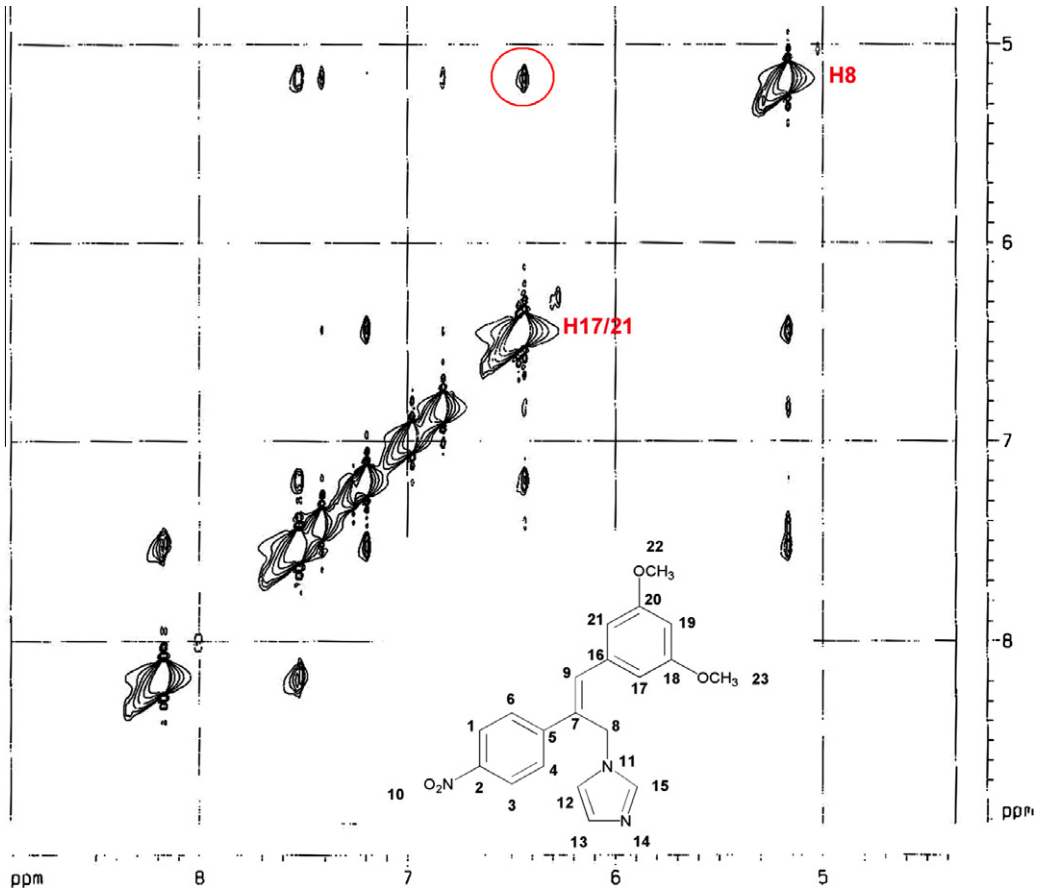

Figure 3. Region of a 2D ^{1}H–^{1}H NOESY spectrum of **82**. The red circle indicates the NOE signal of H8 and H17/21.

4.2.2. 2,4-Dimethoxy-1-vinylbenzene (12)[38]

This compound was prepared in 82% yield by following GP 1. Colorless oil. ^{1}H NMR (300 MHz, $CDCl_3$) δ 7.41 (d, J = 8.4 Hz, 1H), 7.04–6.94 (m, 1H), 6.51–6.45 (m, 2H), 5.65 (d, J = 17.7 Hz, 1H), 5.17 (d, J = 11.4 Hz, 1H), 3.83 (s, 3H), 3.81 (s, 3H).

4.2.3. 1,4-Dimethoxy-2-vinylbenzene (13)[39]

This compound was prepared in 93% yield by following GP 1. Colorless oil. ^{1}H NMR (300 MHz, $CDCl_3$) δ 7.12–7.01 (m, 2H), 6.80 (s, 2H), 5.75 (d, J = 17.7 Hz, 1H), 5.29 (d, J = 8.4 Hz, 1H), 3.80 (s, 3H), 3.79 (s, 3H).

4.2.4. 1,2-Dimethoxy-4-vinylbenzene (14)[39]

This compound was prepared in 87% yield by following GP 1. Colorless oil. ^{1}H NMR (300 MHz, $CDCl_3$) δ 6.95–6.93 (m, 2H), 6.90 (d, J = 1.8 Hz, 1H), 6.69 (dd, J = 17.4 Hz, J = 10.6 Hz, 1H), 5.59 (d, J = 17.4 Hz, 1H), 5.13 (d, J = 10.6 Hz, 1H), 3.88 (s, 3H), 3.85 (s, 3H).

4.2.5. 1,3-Dimethoxy-5-vinylbenzene (15)[40]

This compound was prepared in 93% yield by following GP 1. Colorless oil. ^{1}H NMR (300 MHz, $CDCl_3$) δ 6.59–6.54 (m, 3H), 5.62 (d, J = 17.4 Hz, 1H), 5.16 (d, J = 10.8 Hz, 1H), 3.82–3.81 (m, 9H).

4.2.6. 1,2,3-Trimethoxy-4-vinylbenzene (16)[41]

This compound was prepared in 58% yield by following GP 1. Colorless oil. ^{1}H NMR (300 MHz, $CDCl_3$) δ 7.18 (d, J = 8.7 Hz, 1H), 6.95–6.86 (m, 1H), 6.65 (d, J = 8.7 Hz, 1H), 5.63 (dd, J = 18.0, 1.2 Hz, 1H), 5.17 (dd, J = 18.0, 1.2 Hz, 1H), 3.86 (s, 6H), 3.84 (s, 3H); ^{13}C NMR (75 MHz, $CDCl_3$) δ 153.2, 151.4, 142.2, 130.9, 124.7, 120.5, 113.0, 107.5, 61.1, 60.8, 55.9.

4.2.7. 1,2,5-Trimethoxy-3-vinylbenzene (17)[42]

This compound was prepared in 42% yield by following GP 1. White solid: mp 54–55 °C. ^{1}H NMR (300 MHz, $CDCl_3$) δ 7.02–6.92 (m, 2H), 6.48 (s, 1H), 5.57 (dd, J = 17.7, 1.2 Hz, 1H), 5.13 (dd, J = 14.1, 1.2 Hz, 1H), 3.88 (s, 3H), 3.85 (s, 3H), 3.81 (s, 3H); ^{13}C NMR (75 MHz, $CDCl_3$) δ 151.3, 149.5, 143.2, 130.8, 118.4, 112.0, 109.3, 97.6, 56.6, 56.4, 56.0.

4.2.8. 5-Vinylbenzo[*d*][1,3]dioxole (18)[43]

This compound was prepared in 60% yield by following GP 1. Colorless oil. ^{1}H NMR (300 MHz, $CDCl_3$) δ 6.99 (s, 1H), 6.85 (d, J = 8.1 Hz, 1H), 6.78 (d, J = 8.1 Hz, 1H), 6.64 (dd, J = 16.8 Hz, J = 10.8 Hz, 1H), 5.95 (s, 2H), 5.60 (d, J = 16.8 Hz, 1H), 5.15 (d, J = 10.8 Hz, 1H); ^{13}C NMR (75 MHz, $CDCl_3$) δ 147.9, 147.3, 136.3, 132.0, 120.9, 111.8, 108.0, 105.3, 100.9.

4.2.9. 1,2,3-Trimethoxy-5-vinylbenzene (19)[40]

This compound was prepared in 85% yield by following GP 1. Colorless oil. ^{1}H NMR (300 MHz, $CDCl_3$) δ 6.59–6.54 (m, 3H), 5.62 (d, J = 17.8 Hz, 1H), 5.16 (d, J = 10.8 Hz, 1H), 3.82–3.81 (m, 9H).

4.2.10. 1-Methoxy-3-vinylbenzene (20)[44]

This compound was prepared in 73% yield by following GP 1. Colorless oil. ^{1}H NMR (300 MHz, $CDCl_3$) δ 6.95–6.93 (m, 2H), 6.90 (d, J = 1.8 Hz, 1H), 6.69 (dd, J = 17.4 Hz, J = 10.6 Hz, 1H), 5.59 (d, J = 17.4 Hz, 1H), 5.13 (d, J = 10.6 Hz, 1H), 3.88 (s, 3H), 3.85 (s, 3H).

4.2.11. 3,5-Dimethoxy-4′-amino-*trans*-stilbene (32)

This compound was prepared in 64% yield by following GP 2. Yellow solid: mp 90–91 °C. IR (film) 3369, 1595, 1516, 1456,

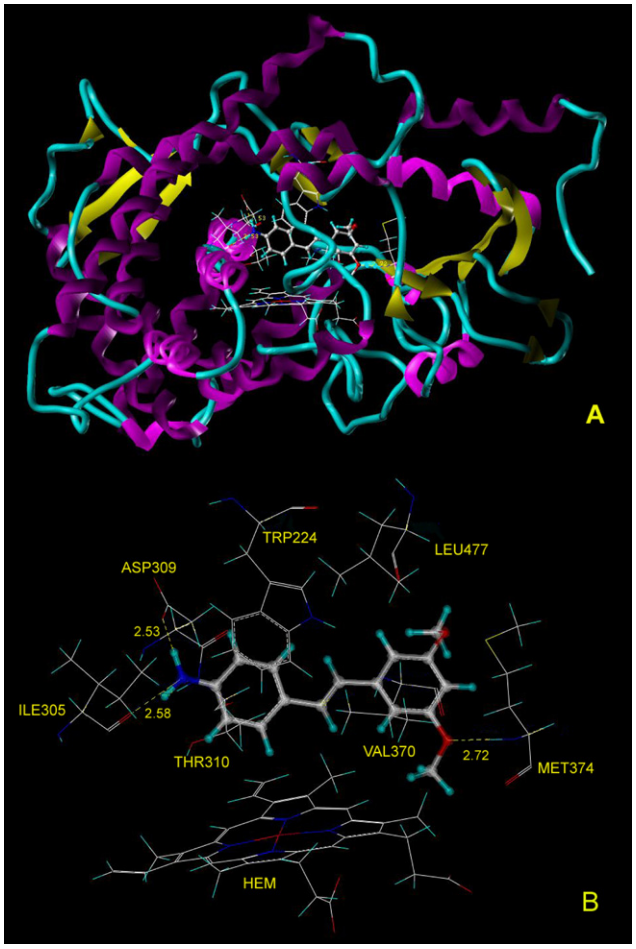

Figure 4. (A) Ribbon diagram illustrating the hypothetical complex structure of human aromatase with compound **32** bound to the active site, and the hydrogen bonds are labeled as yellow broken lines. (B) Potential interactions between compound **32** and Ile305, Asp309, Thr310, Trp224, Val370, Met374 in human aromatase active site. The hydrogen bonds are labeled as yellow broken lines.

1203, 1151, 1066, 962 cm^{-1}; ^1H NMR (300 MHz, $CDCl_3$) δ 7.31 (d, J = 8.4 Hz, 2H), 6.99 (d, J = 16.2 Hz, 1H), 6.83 (d, J = 16.2 Hz, 1H), 6.65 (d, J = 8.4 Hz, 2H), 6.62 (d, J = 2.1 Hz, 2H), 6.34 (t, J = 2.1 Hz, 1H), 3.81 (s, 6H), 3.75 (br, 2H); ^{13}C NMR (75 MHz, $CDCl_3$) δ 160.8, 146.2, 139.9, 129.1, 127.7, 124.9, 115.1, 104.0, 99.2, 55.3; CIMS 256 (MH^+); HRMS calcd for $C_{16}H_{17}O_2N$ *m/z* 255.1259, found: *m/z* 255.1261 (M^+).

4.2.12. 2,4-Dimethoxy-4′-amino-*trans*-stilbene (33)

This compound was prepared in 59% yield by following GP 2. Yellow solid: mp 97–98 °C. IR (film) 3372, 1609, 1577, 1517, 1464, 1286, 1207, 968 cm^{-1}; ^1H NMR (300 MHz, $CDCl_3$) δ 7.48 (d, J = 8.4 Hz, 1H), 7.34 (d, J = 8.4 Hz, 2H), 7.22 (d, J = 16.5 Hz, 1H), 6.93 (d, J = 16.5 Hz, 1H), 6.66 (d, J = 8.4 Hz, 2H), 6.49–6.46 (m, 2H), 3.85 (s, 3H), 3.82 (s, 3H); ^{13}C NMR (75 MHz, $CDCl_3$) δ 159.9, 157.6, 145.3, 129.1, 127.4, 127.0, 126.6, 120.0, 119.6, 115.3, 104.8, 98.4, 55.4, 55.3; CIMS *m/z* 256 (MH^+); HRMS calcd for $C_{16}H_{18}O_2N$ *m/z* 256.1338, found: *m/z* 256.1344 (MH^+).

4.2.13. 2,4-Dimethoxy-3′-amino-*trans*-stilbene (34)

This compound was prepared in 42% yield by following GP 2. Yellow solid: mp 69–70 °C. IR (film) 3369, 1598, 1577, 1504, 1456, 1287, 1158, 971 cm^{-1}; ^1H NMR (300 MHz, $CDCl_3$) δ 7.49 (d, J = 8.4 Hz, 1H), 7.35 (d, J = 16.5 Hz, 1H), 7.11 (t, J = 7.8 Hz, 1H), 6.94–6.86 (m, 3H), 6.57 (dd, J = 2.1 Hz, 8.1 Hz, 1H), 6.50 (dd, J = 2.4 Hz, 8.7 Hz, 1H), 6.46 (d, J = 2.4 Hz, 1H), 3.85 (s, 3H), 3.82 (s, 3H), 3.77 (br, 2H); ^{13}C NMR (75 MHz, $CDCl_3$) δ 160.4, 157.9, 146.1, 139.3, 129.4, 127.1, 127.0, 123.0, 119.5, 117.4, 114.2, 112.8, 104.9, 98.4, 55.4, 55.3; ESIMS *m/z* 256 (MH^+); HRMS calcd for $C_{16}H_{18}O_2N$ *m/z* 256.1338, found: *m/z* 256.1340 (MH^+).

4.2.14. 2,5-Dimethoxy-4′-amino-*trans*-stilbene (35)[45]

This compound was prepared in 35% yield by following GP 2. Yellow solid: mp 91–92 °C. IR (film) 3370, 1601, 1516, 1493, 1282, 1215, 1046, 969 cm^{-1}; ^1H NMR (300 MHz, $CDCl_3$) δ 7.36 (d, J = 8.4 Hz, 2H), 7.27 (d, J = 16.2 Hz, 1H), 7.11 (d, J = 2.7 Hz, 1H), 6.99 (d, J = 16.2 Hz, 1H), 6.81 (d, J = 8.7 Hz, 1H), 6.76 (d, J = 2.7 Hz, 1H), 6.71 (d, J = 8.4 Hz, 2H), 4.15 (br, 2H), 3.82 (s, 3H), 3.80 (s, 3H); ^{13}C NMR (75 MHz, $CDCl_3$) δ 153.7, 151.1, 146.0, 129.3, 128.3, 127.8, 119.4, 115.1, 112.8, 112.2, 111.1, 56.2, 55.7; CIMS *m/z* 256 (MH^+).

4.2.15. 2,3-Dimethoxy-4′-amino-*trans*-stilbene (36)

This compound was prepared in 75% yield by following GP 2. Yellow solid: mp 97–98 °C. IR (film) 3367, 2923, 1539, 1515, 1343, 961 cm^{-1}; ^1H NMR (300 MHz, $CDCl_3$) δ 7.37 (d, J = 8.1 Hz, 2H), 7.29 (d, J = 16.8 Hz, 1H), 7.21 (dd, J = 1.2 Hz, 7.8 Hz, 1H), 7.07–7.02 (m, 2H), 6.82–6.77 (m, 3H), 3.88 (s, 3H), 3.84 (s, 3H); ^{13}C NMR (75 MHz, $CDCl_3$) δ 152.8, 146.3, 146.1, 131.9, 129.8, 128.0, 127.7, 123.9, 118.8, 117.3, 115.0, 110.4, 60.8, 55.6; ESIMS *m/z* 256 (MH^+); HRMS calcd for $C_{16}H_{17}O_2N$ *m/z* 255.1259, found: *m/z* 255.1257 (M^+).

4.2.16. (3,4-Dimethoxy-4′-amino-*trans*-stilbene (37)[46]

This compound was prepared in 75% yield by following GP 2. Yellow solid: mp 158–159 °C. IR (film) 3368, 1622, 1604, 1516,

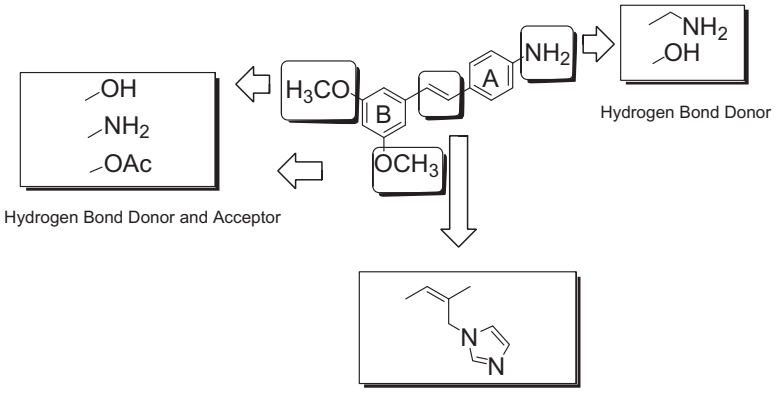

Figure 5. Design of the novel resveratrol analogues based on the docking result of compound **32**.

Table 2
Inhibition of the human aromatase by resveratrol analogues

Compd	% Inhib[a] (20 μg/mL)	IC_{50}[b] (μM)	Compd	% Inhib[a] (20 μg/mL)	IC_{50}[b] (μM)	Compd	% Inhib[a] (20 μg/mL)	IC_{50}[b] (μM)
32	92.91	0.59 ± 0.07	**47**	77.6	21.86 ± 0.44	**62**	89.67	2.79 ± 0.11
33	91.14	0.76 ± 0.04	**48**	81.80	8.49 ± 0.08	**63**	87.01	3.21 ± 0.09
34	76.27	11.14 ± 3.09	**49**	63.71	8.33 ± 0.81	**64**	88.68	7.47 ± 0.79
35	80.94	1.82 ± 0.03	**50**	38.08	N/T[c]	**65**	88.04	8.51 ± 0.64
36	91.22	0.98 ± 0.12	**51**	89.90	3.08 ± 0.44	**66**	13.18	N/T[c]
37	78.93	14.51 ± 0.20	**52**	4.21	N/T[c]	**67**	23.52	N/T[c]
38	31.38	N/T[c]	**53**	0	N/T[c]	**72**	86.39	2.94 ± 0.43
39	5.33	N/T[c]	**54**	44.25	N/T[c]	**73**	35.82	N/T[c]
40	7.56	N/T[c]	**55**	22.19	N/T[c]	**74**	94.01	5.0 ± 1.17
41	6.74	N/T[c]	**56**	19.65	N/T[c]	**75**	45.23	N/T[c]
42	83.50	16.42 ± 0.21	**57**	15.38	N/T[c]	**80**	94.92	0.19 ± 0.08
43	12.01	N/T[c]	**58**	14.65	N/T[c]	**81**	94.20	1.84 ± 0.02
44	90.86	0.90 ± 0.08	**59**	18.33	N/T[c]	**82**	91.4	0.07 ± 0.02
45	88.94	3.57 ± 0.11	**60**	90.66	2.76 ± 0.33	**84**	93.6	0.036 ± 0.003
46	81.26	2.28 ± 0.28	**61**	92.49	0.67 ± 0.07			

[a] The inhibition percentage was tested at a concentration of 20 μg/mL of each compound.
[b] The IC_{50} values (μM) are the concentrations corresponding to 50% inhibition of aromatase.
[c] N/T means not tested (in general, compounds with low percent inhibitions in the initial screening at 20 μg/mL were not evaluated more extensively to determine their IC_{50} values).

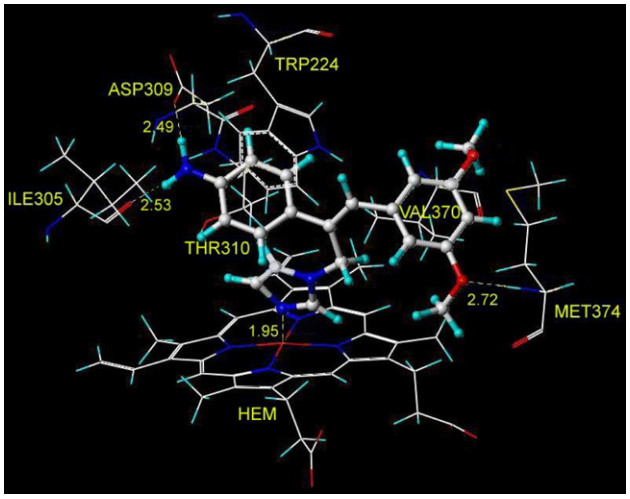

Figure 6. Potential interactions between compound **84** and Ile305, Asp309, Thr310, Trp224, Val370, Met374 and heme in human aromatase active site. The hydrogen bonds are labeled as yellow broken lines.

Table 3
K_M and V_{max} values for resveratrol analogues active as inhibitors of aromatase[a]

Compd	K_M (μM)	V_{max}
32	7.44 ± 0.06	35.2 ± 0.33
33	10.68 ± 0.19	35.6 ± 0.18
34	2.87 ± 0.08	35.1 ± 0.31
35	8.21 ± 0.24	34.2 ± 0.21
36	5.92 ± 0.14	34.8 ± 0.41
37	2.57 ± 0.13	34.8 ± 0.15
42	2.35 ± 0.10	34.4 ± 0.26
44	6.25 ± 0.11	35.4 ± 0.27
45	7.48 ± 0.17	34.9 ± 0.34
46	9.31 ± 0.21	34.6 ± 0.29
47	2.19 ± 0.05	34.9 ± 0.24
48	7.59 ± 0.09	35.1 ± 0.29
49	6.94 ± 0.07	34.8 ± 0.29
51	8.75 ± 0.16	35 ± 0.08
60	8.35 ± 0.13	34.8 ± 0.25
61	8.72 ± 0.18	34.7 ± 0.16
62	8.53 ± 0.16	34.7 ± 0.26
63	6.99 ± 0.20	34.9 ± 0.30
64	7.83 ± 0.14	35.3 ± 0.18
65	7.81 ± 0.13	35 ± 0.22
72	8.21 ± 0.09	35.2 ± 0.22
74	6.54 ± 0.15	34.3 ± 0.35
80	12.78 ± 0.14	35.1 ± 0.17
81	8.76 ± 0.20	34.7 ± 0.21
82	15.2 ± 0.23	35.5 ± 0.28
84	16.42 ± 0.17	34.4 ± 0.33

[a] The IC_{50} values are listed in Table 2.

1465, 1137, 1023, 965 cm^{-1}; ^1H NMR (300 MHz, $CDCl_3$) δ 7.32 (d, J = 8.4 Hz, 2H), 7.04 (d, J = 1.8 Hz, 1H), 7.00 (dd, J = 1.8 Hz, 8.1 Hz, 1H), 6.88 (s, 1H), 6.83 (d, J = 8.1 Hz, 1H), 6.67 (d, J = 8.4 Hz, 2H), 3.92 (s, 3H), 3.87 (s, 3H), 3.75 (br, 2H); ^{13}C NMR (75 MHz, $CDCl_3$) δ 149.0, 148.3, 145.8, 131.0, 128.1, 127.4, 126.8, 124.8, 119.2, 115.2, 111.1, 108.3, 55.8, 55.7; CIMS m/z 256 (MH^+).

4.2.17. 3,4-Dimethoxy-4′-cyano-*trans*-stilbene (38)

This compound was prepared in 61% yield by following GP 2. Yellow solid: mp 102–103 °C. IR (film) 3398, 2223, 1595, 1515, 1463, 1267, 1139, 964 cm^{-1}; ^1H NMR (300 MHz, $CDCl_3$) δ 7.60 (d, J = 8.4 Hz, 2H), 7.53 (d, J = 8.4 Hz, 2H), 7.14 (d, J = 16.5 Hz, 1H), 7.06 (d, J = 6.3 Hz, 2H), 6.93 (d, J = 16.5 Hz, 1H), 6.86 (d, J = 9.0 Hz, 1H), 3.93 (s, 3H), 3.90 (s, 3H); ^{13}C NMR (75 MHz, $CDCl_3$) δ 149.6, 149.1, 142.0, 132.4, 132.1, 129.2, 126.5, 124.6, 120.6, 119.0, 111.1, 110.0, 108.8, 55.9; CIMS m/z 266 (MH^+); HRMS calcd for $C_{17}H_{15}O_2N$ m/z 265.1103, found: m/z 265.1100 (M^+).

4.2.18. 3,4-Dimethoxy-4′-acetoxy-*trans*-stilbene (39)[47]

This compound was prepared in 59% yield by following GP 2. Yellow solid: mp 125–126 °C. IR (film) 3368, 2927, 1760, 1515, 1420, 1196, 964 cm^{-1}; ^1H NMR (300 MHz, $CDCl_3$) δ 7.47 (d, J = 8.4 Hz, 2H), 7.07–6.97 (m, 5H), 6.93 (d, J = 16.5 Hz, 1H), 6.83 (d, J = 7.8 Hz, 1H), 3.93 (s, 3H), 3.89 (s, 3H), 2.29 (s, 3H); ^{13}C NMR (75 MHz, $CDCl_3$) δ 169.5, 149.7, 149.1, 135.3, 130.2, 128.7, 127.1, 125.7, 121.7, 119.9, 111.1, 108.6, 55.9, 55.8, 21.1; CIMS m/z 299 (MH^+).

4.2.19. 3,4-Dimethoxy-4′-fluoro-*trans*-stilbene (40)

This compound was prepared in 57% yield by following GP 2. Yellow solid: mp 117–118 °C. IR (film) 3368, 1600, 1515, 1461, 1225, 1139, 1022, 964 cm^{-1}; ^1H NMR (300 MHz, $CDCl_3$) δ 7.45 (dd, J = 5.7 Hz, 8.4 Hz, 2H), 7.07–7.02 (m, 4H), 6.97 (d, J = 16.5 Hz, 1H), 6.91 (d, J = 16.5 Hz, 1H), 6.86 (d, J = 7.8 Hz, 1H), 3.95 (s, 3H), 3.90 (s, 3H); ^{13}C NMR (75 MHz, $CDCl_3$) δ148.9, 133.6, 130.2, 128.2, 127.7, 127.5, 125.5, 119.7, 115.6, 115.3, 111.1, 108.5, 55.8, 55.7; CIMS m/z 259 (MH^+); HRMS calcd for $C_{16}H_{15}O_2F$ m/z 258.1056, found: m/z 258.1051 (M^+).

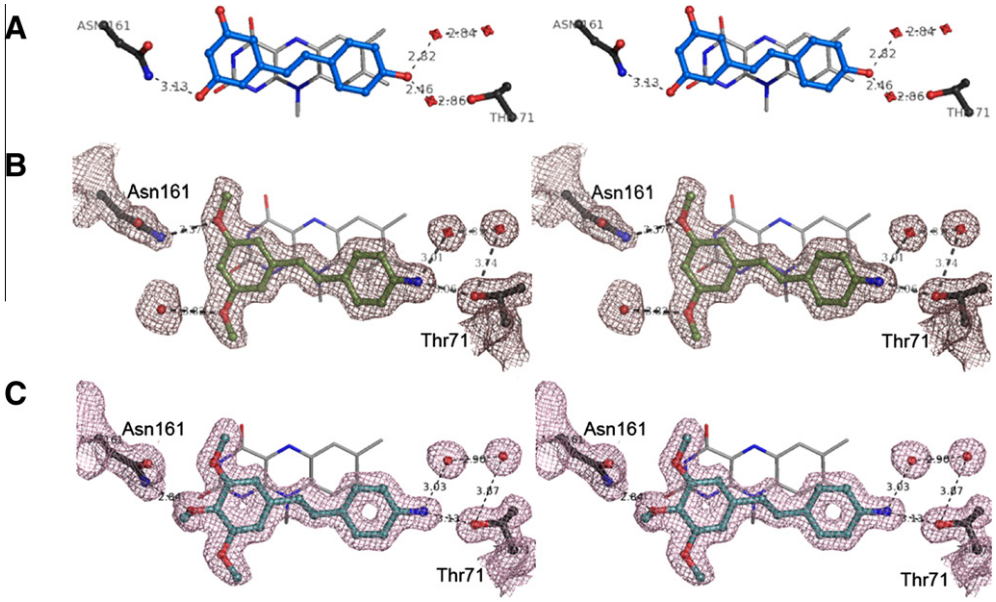

Figure 7. High-resolution X-ray structures of human QR2 in complex with resveratrol (A), compound **32** (B), and compound **44** (C). All panels are presented in walleyed stereoviews showing the FAD cofactor and the active site residues Asn161 and Thr71. Active site water molecules are shown as red spheres and hydrogen bonds are shown as dashed lines. $2F_o - F_c$ electron density maps are contoured to 1 σ. Carbon atoms and bonds are colored blue for resveratrol, green for compound **32** and cyan for compound **44**. The X-ray structure of the QR2-resveratrol complex is from PDB code 1SG0.[22]

4.2.20. 3,4,5-Trimethoxy-4′-nitro-*trans*-stilbene (41)[48]

This compound was prepared in 68% yield by following GP 2. Orange solid: mp 192–193 °C. IR (film) 1594, 1581, 1506, 1331, 1265, 1126,1108 cm^{-1}; ^1H NMR (300 MHz, $CDCl_3$) δ 8.20 (d, J = 8.7 Hz, 2H), 7.61 (d, J = 8.7 Hz, 2H), 7.18 (d, J = 16.2 Hz, 1H), 7.03 (d, J = 16.2 Hz, 1H), 6.76 (s, 2H), 3.91 (s, 6H), 3.87 (s, 3H); ^{13}C NMR (75 MHz, $CDCl_3$) δ 153.5, 146.7, 143.8, 133.3, 131.8, 126.7, 125.7, 124.2, 104.1, 61.0, 56.2; CIMS m/z 316 (MH^+).

4.2.21. 3,4,5-Trimethoxy-4′-amino-*trans*-stilbene (42)

This compound was prepared in 52% yield by following GP 2. Yellow solid: mp 105–106 °C. IR (film) 3367, 2926, 1599, 1583, 1505, 1457, 1417, 1243, 1126, 959 cm^{-1}; ^1H NMR (300 MHz, $CDCl_3$) δ 7.13 (t, J = 7.5 Hz, 1H), 7.11 (d, J = 16.2 Hz, 1H), 6.92–6.87 (m, 2H), 6.81 (s, 1H), 6.71 (s, 2H), 6.57 (dd, J = 7.8, 1.8 Hz, 1H), 3.89 (s, 6H), 3.86 (s, 3H), 3.66 (br, 2H); ^{13}C NMR (75 MHz, $CDCl_3$) δ 153.3, 146.6, 138.1, 137.7, 133.1, 129.5, 128.3, 117.1, 114.6, 112.7, 103.4, 60.9, 56.0. ESIMS m/z 286 (MH^+); HRMS calcd for $C_{17}H_{20}O_3N$ m/z 286.1443, found: m/z 286.1446 (MH^+).

4.2.22. 3,4,5-Trimethoxy-4′-aminomethyl-*trans*-stilbene (43)

This compound was prepared in 57% yield by following GP 2. White solid: mp 139–140 °C. IR (film) 3341, 2937, 1672, 1583, 1508, 1462, 1421, 1237, 1125, 964 cm^{-1}; ^1H NMR (300 MHz, $CDCl_3$) δ 7.45 (d, J = 8.1 Hz, 2H), 7.25 (d, J = 8.1 Hz, 2H), 7.02 (d, J = 16.2 Hz, 1H), 6.95 (d, J = 16.2 Hz, 1H), 6.7 (s, 2H), 4.47 (d, J = 5.7 Hz, 2H), 3.90 (s, 6H), 3.86 (s, 3H); ^{13}C NMR (75 MHz, $CDCl_3$) δ 161.0, 153.3, 136.8, 136.6, 132.8, 128.8, 128.1, 127.4, 126.6, 103.4, 60.9, 56.0, 41.8; ESIMS m/z 283 $(MH-NH_3)^+$; HRMS calcd for $C_{18}H_{19}O_3$ m/z 283.1334, found: m/z 283.1336 $(MH-NH_3)^+$.

4.2.23. 3,4,5-Trimethoxy-4′-amino-*trans*-stilbene (44)

This compound was prepared in 50% yield by following GP 2. Yellow solid: mp 135–136 °C. IR (film) 3368, 1606, 1580, 1516, 1417, 1234, 1124, 959 cm^{-1}; ^1H NMR (300 MHz, $CDCl_3$) δ 7.33 (d, J = 8.4 Hz, 2H), 6.92 (d, J = 16.2 Hz, 1H), 6.83 (d, J = 16.2 Hz, 1H), 6.73 (d, J = 8.4 Hz, 2H), 6.68 (s, 2H), 3.89 (s, 6H), 3.86 (s, 3H); ^{13}C NMR (75 MHz, $CDCl_3$) δ 153.3, 146.1, 137.2, 133.7, 128.2, 127.6, 124.9, 115.1, 114.5, 103.0, 60.9, 56.0; CIMS m/z 286 (MH^+); HRMS calcd for $C_{17}H_{20}O_3N$ m/z 286.1443, found: m/z 286.1442 (MH^+).

4.2.24. 2,3,4-Trimethoxy-4′-amino-*trans*-stilbene (45)

This compound was prepared in 31% yield by following GP 2. Yellow solid: mp 139–140 °C. IR (film) 3369, 1606, 1516, 1493, 1413, 1297, 1094, 969 cm^{-1}; ^1H NMR (300 MHz, $CDCl_3$) δ 7.28 (d, J = 8.4 Hz, 2H), 7.21 (d, J = 1.2 Hz, 1H), 7.09 (d, J = 16.5 Hz, 1H), 6.88 (d, J = 16.5 Hz, 1H), 6.65–6.61 (m, 3H), 3.84 (s, 3H), 3.84 (s, 3H), 3.82 (s, 3H), 3.69 (br, 2H); ^{13}C NMR (75 MHz, $CDCl_3$) δ 152.6, 151.3, 145.7, 142.3, 128.6, 127.9, 127.5, 125.0, 120.1, 119.2, 115.1, 107.7, 61.2, 60.8, 56.0; ESIMS m/z 286 (MH^+); HRMS calcd for $C_{17}H_{20}O_3N$ m/z 286.1443, found: m/z 286.1441 (MH^+).

4.2.25. 2,3,5-Trimethoxy-4′-amino-*trans*-stilbene (46)

This compound was prepared in 38% yield by following GP 2. Yellow solid: mp 105–106 °C. IR (film) 3369, 1608, 1518, 1464, 1206, 1032, 965 cm^{-1}; ^1H NMR (300 MHz, $CDCl_3$) δ 7.33 (d, J = 8.4 Hz, 2H), 7.21 (d, J = 16.2 Hz, 1H), 7.08 (s, 1H), 6.86 (d, J = 16.2 Hz, 1H), 6.65 (d, J = 8.4 Hz, 2H), 6.51 (s, 1H), 3.89 (s, 6H), 3.84 (s, 3H), 3.69 (br, 2H); ^{13}C NMR (75 MHz, $CDCl_3$) δ 151.2, 148.9, 145.6, 143.3, 128.8, 127.4, 126.9, 119.3, 118.9, 115.1, 109.0, 97.8, 56.7, 56.4, 56.0; ESIMS m/z 286 (MH^+); HRMS calcd for $C_{17}H_{20}O_3N$ m/z 286.1443, found: m/z 286.1442 (MH^+).

4.2.26. (*E*)-3-(2-(Benzo[*d*][1,3]dioxol-5-yl)vinyl)benzenamine (47)

This compound was prepared in 66% yield by following GP 2. Yellow solid: mp 86–87 °C. IR (film) 3377, 1599, 1500, 1486, 1444, 1251, 1035, 963 cm^{-1}; ^1H NMR (300 MHz, $CDCl_3$) δ 7.14 (t, J = 7.8 Hz, 1H), 7.05 (d, J = 1.5 Hz, 1H), 7.00, (d, J = 16.2 Hz, 1H), 6.94–6.89 (m, 2H), 6.85 (d, J = 16.2 Hz, 1H), 6.80 (d, J = 8.1 Hz, 2H), 6.59 (dd, J = 7.8 Hz, 1.5 Hz, 1H), 5.97 (s, 2H), 3.69 (s, 2H); ^{13}C NMR (75 MHz, $CDCl_3$) δ 148.0, 147.1, 146.5, 138.4, 131.8, 129.5, 128.1, 127.1, 121.3, 117.0, 114.3, 112.6, 108.3, 105.4, 101.0; CIMS m/z 240 (MH^+); HRMS calcd for $C_{15}H_{13}O_2N$ m/z 239.0946, found: m/z 239.0945 (M^+).

4.2.27. (*E*)-4-(2-(Benzo[*d*][1,3]dioxol-5-yl)vinyl)benzenamine (48)

This compound was prepared in 75% yield by following GP 2. Yellow solid: mp 132–133 °C. IR (film) 3368, 2924, 1606, 1516, 1489, 1446, 1253, 1038, 960 cm^{-1}; ^1H NMR (500 MHz, $CDCl_3$) δ 7.30 (d, J = 8.4 Hz, 2H), 7.03 (d, J = 1.5 Hz, 1H), 6.89 (dd, J = 8.4 Hz, 1.5 Hz, 1H), 6.87 (d, J = 16.2 Hz, 1H), 6.82 (d, J = 16.2 Hz, 1H), 6.78 (d, J = 8.1 Hz, 1H), 6.66 (d, J = 8.4 Hz, 2H), 5.96 (s, 2H), 3.73 (br, 2H); ^{13}C NMR (125 MHz, $CDCl_3$) δ 148.0, 146.6, 145.8, 132.4, 128.0, 127.4, 127.0, 124.7, 120.7, 115.1, 108.3, 105.2, 100.9; ESIMS m/z 240 (MH^+); HRMS calcd for $C_{15}H_{14}O_2N$ m/z 240.1025, found: m/z 240.1022 (MH^+).

4.2.28. 3-Nitro-4′-nitro-*trans*-stilbene (49)[49]

This compound was prepared in 46% yield by following GP 2. Yellow solid: mp 224–226 °C. IR (film) 1593, 1524, 1514, 1356, 1340, 972, 960, 868 cm^{-1}; ^1H NMR (300 MHz, $CDCl_3$) δ 8.40 (t, J = 1.5 Hz, 1H), 8.25 (d, J = 9.0 Hz, 2H), 8.16 (d, J = 8.1 Hz, 1H), 7.82 (d, J = 7.8 Hz, 1H), 7.67 (d, J = 9.0 Hz, 2H), 7.57 (t, J = 7.8 Hz, 1H), 7.30 (d, J = 16.5 Hz, 1H), 7.24 (d, J = 16.5 Hz, 1H); ^{13}C NMR (75 MHz, $CDCl_3$) δ 148.7, 147.3, 142.5, 137.9, 132.6, 130.4, 129.8, 129.2, 127.2, 124.2, 123.0, 121.2; ESIMS m/z 271 (MH^+).

4.2.29. 3-Nitro-4′-amino-*trans*-stilbene (50)

This compound was prepared in 39% yield by following GP 2. Yellow solid: mp 177–178 °C. IR (film) 3469, 3390, 1620, 1527, 1356, 970, 819 cm^{-1}; ^1H NMR (300 MHz, $CDCl_3$) δ 8.29 (s, 1H), 8.01 (d, J = 6.6 Hz, 1H), 7.72 (d, J = 7.8 Hz, 1H), 7.46 (t, J = 7.8 Hz, 1H), 7.34 (d, J = 8.4 Hz, 2H), 7.12 (d, J = 16.5 Hz, 1H), 6.91 (d, J = 16.5 Hz, 1H), 6.67 (d, J = 8.4 Hz, 2H), 3.81 (s, 2H); ^{13}C NMR (75 MHz, $CDCl_3$) δ 150.4, 149.3, 141.1, 133.0, 132.6, 130.9, 129.2, 124.9, 121.6, 121.2, 120.7, 114.7; CIMS m/z 241 (MH^+); HRMS calcd for $C_{14}H_{12}O_2N_2$ m/z 240.0899, found: m/z 240.0898 (M^+).

4.2.30. 3-Methoxyl-4′-amino-*trans*-stilbene (51)[50]

This compound was prepared in 51% yield by following GP 2. Yellow solid: mp 70–71 °C. IR (film) 2917, 1666, 1601, 1518, 1289, 965 cm^{-1}; ^1H NMR (300 MHz, $CDCl_3$) δ 7.37 (d, J = 8.4 Hz, 2H), 7.30 (t, J = 7.8 Hz, 1H), 7.14–7.05 (m, 3H), 6.95 (d, J = 16.2 Hz, 1H), 6.83 (dd, J = 2.1 Hz, 7.8 Hz, 1H), 6.69 (d, J = 7.8 Hz, 2H), 3.87 (s, 3H), 3.75 (br, 1H); ^{13}C NMR (75 MHz, $CDCl_3$) δ 159.8, 146.3, 139.4, 129.5, 129.0, 127.8, 124.8, 118.8, 115.2, 112.5, 111.3, 55.2; ESIMS m/z 226 (MH^+).

4.2.31. 3,5-Dinitro-4′-nitro-*trans*-stilbene (52)

This compound was prepared in 42% yield by following GP 2. Yellow solid: mp 281–282 °C. IR (film) 3368, 1533, 1506, 1343, 1331, 961 cm^{-1}; ^1H NMR (300 MHz, DMSO-d_6) δ 8.90 (d, J = 2.1 Hz, 2H), 8.72 (t, J = 1.8 Hz, 1H), 8.29 (d, J = 9.0 Hz, 2H), 7.94–7.88 (m, 3H), 7.81 (d, J = 16.5 Hz, 1H); ^{13}C NMR (75 MHz, DMSO-d_6) δ 149.5, 147.9, 143.7, 141.0, 132.5, 130.0, 129.0, 127.6, 125.1, 118.4; negative ion ESIMS m/z 314 $(M-H^+)^-$; negative ion HRMS calcd for $C_{14}H_8O_6N_3$ m/z 314.0413, found: m/z 314.0418 $(M-H^+)^-$.

4.2.32. 3,5-Dimethoxyl-4′-amino-*trans*-stilbene (53)[51]

This compound was prepared in 67% yield by following GP 2. Yellow solid: mp 134–135 °C. IR (film) 3368, 1588, 1509, 1462, 1336, 1205, 1164, 1064, 952 cm^{-1}; ^1H NMR (300 MHz, $CDCl_3$) δ 8.20 (d, J = 8.7 Hz, 2H), 7.61 (d, J = 8.7 Hz, 2H), 7.18 (d, J = 16.2 Hz, 1H), 7.09 (d, J = 16.2 Hz, 1H), 6.68 (d, J = 1.8 Hz, 2H), 6.43 (t, J = 2.1 Hz, 1H), 3.83 (s, 6H); ^{13}C NMR (75 MHz, $CDCl_3$) δ 160.7, 133.8, 129.7, 128.2, 126.8, 123.4, 106.6, 105.0, 100.9, 100.0, 55.2; CIMS m/z 286 (MH^+).

4.2.33. 3,5-Dimethoxyl-3′-amino-*trans*-stilbene (54)

This compound was prepared in 44% yield by following GP 2. Yellow solid: mp 72–73 °C. IR (film) 3368, 1599, 1590, 1459, 1204, 1152, 1065, 960 cm^{-1}; ^1H NMR (300 MHz, $CDCl_3$) δ 7.16 (t, J = 7.8 Hz, 1H), 7.00 (s, 2H), 6.93 (d, J = 7.8 Hz, 1H), 6.84 (t, J = 2.1 Hz, 1H), 6.67 (d, J = 2.4 Hz, 2H), 6.61 (dd, J = 2.4 Hz, 8.4 Hz, 1H), 6.41 (t, J = 2.1 Hz, 1H), 3.84 (s, 6H); ^{13}C NMR (75 MHz, $CDCl_3$) δ 160.9, 146.6, 139.4, 138.1, 129.5, 129.3, 128.4, 117.3, 114.7, 112.8, 104.5, 99.8, 55.3; ESIMS m/z 256 (MH^+). HRMS calcd for $C_{16}H_{17}O_2N$ m/z 256.1338, found: m/z 256.1341 (MH^+).

4.2.34. 3,5-Dimethoxy-4′-acetoxy-*trans*-stilbene (55)[52]

This compound was prepared in 50% yield by following GP 2. White solid: mp 121–122 °C. IR (film) 3399, 1759, 1591, 1505, 1457, 1194, 1152, 968 cm^{-1}; ^1H NMR (300 MHz, $CDCl_3$) δ 7.49 (d, J = 8.7 Hz, 2H), 7.09–7.02 (m, 3H), 6.96 (d, J = 16.5 Hz, 1H), 6.64 (d, J = 2.1 Hz, 2H), 6.39 (t, J = 2.4 Hz, 1H), 3.82 (s, 6H), 2.29 (s, 3H); ^{13}C NMR (75 MHz, $CDCl_3$) δ 169.4, 160.9, 150.1, 139.1, 134.9, 128.9, 128.1, 127.5, 121.8, 104.5, 100.0, 55.3, 21.1; CIMS m/z 299 (MH^+).

4.2.35. 3,5-Dimethoxy-4′-aminomethyl-*trans*-stilbene (56)

This compound was prepared in 50% yield by following GP 2. White solid: mp 115–116 °C. IR (film) 3292, 2927, 1660, 1593, 1457, 1426, 1204, 1151, 1067, 963 cm^{-1}; ^1H NMR (300 MHz, $CDCl_3$) δ 7.46 (d, J = 8.4 Hz, 2H), 7.26 (d, J = 8.4 Hz, 2H), 7.06 (d, J = 16.5 Hz, 1H), 6.99 (d, J = 16.5 Hz, 1H), 6.65 (d, J = 2.1 Hz, 2H), 6.39 (t, J = 2.1 Hz, 1H), 5.92 (br, 1H), 4.47 (d, J = 6.0 Hz, 2H), 3.82 (s, 6H); ^{13}C NMR (75 MHz, $CDCl_3$) δ 160.9, 139.0, 136.9, 136.6, 128.8, 128.4, 128.1, 126.8, 104.5, 100.0, 55.3, 41.8; ESIMS m/z 253 $(MH-NH_3)^+$; HRMS calcd for $C_{17}H_{17}O_2$ m/z 253.1229, found: m/z 253.1228 $(MH-NH_3)^+$.

4.2.36. 3,5-Dimethoxy-4′-fluoro-*trans*-stilbene (57)[53]

This compound was prepared in 56% yield by following GP 2. White solid: mp 44–45 °C. IR (film) 1597, 1509, 1457, 1228, 1204, 1157, 1067, 962 cm^{-1}; ^1H NMR (300 MHz, $CDCl_3$) δ 7.48–7.43 (m, 2H), 7.06–7.00 (m, 3H), 6.93 (d, J = 16.2 Hz, 1H), 6.64 (d, J = 2.4 Hz, 2H), 6.39 (t, J = 2.1 Hz, 1H), 3.82 (s, 6H); ^{13}C NMR (75 MHz, $CDCl_3$) δ 160.9, 139.1, 133.2, 128.3, 128.0, 127.9, 115.7, 115.4, 104.4, 99.8, 55.3; ESIMS m/z 259 (MH^+).

4.2.37. 3,5-Dimethoxyl-4′-chloro-*trans*-stilbene (58)[54]

This compound was prepared in 57% yield by following GP 2. White solid: mp 65–66 °C. IR (film) 3369, 1587, 1455, 1347, 1206, 1151, 1057, 956 cm^{-1}; ^1H NMR (300 MHz, $CDCl_3$) δ 7.41 (d, J = 8.7 Hz, 2H), 7.30 (d, J = 8.7 Hz, 2H), 7.02 (d, J = 16.8 Hz, 1H), 6.97 (d, J = 16.8 Hz, 1H), 6.64 (d, J = 2.4 Hz, 2H), 6.39 (t, J = 2.1 Hz, 1H), 3.81 (s, 6H); ^{13}C NMR (75 MHz, $CDCl_3$) δ 160.9, 138.8, 135.5, 133.2, 129.2, 128.89, 127.8, 127.6, 104.5, 100.1, 55.3; ESIMS m/z 275 (MH^+).

4.2.38. 3,5-Dimethoxy-4′-cyano-*trans*-stilbene (59)

This compound was prepared in 63% yield by following GP 2. White solid: mp 106–107 °C. IR (film) 3400, 2223, 1602, 1586, 1458, 1427, 1206, 1154, 1061, 948 cm^{-1}; ^1H NMR (300 MHz, $CDCl_3$) δ 7.60 (d, J = 8.1 Hz, 2H), 7.53 (d, J = 8.1 Hz, 2H), 7.11 (d, J = 16.2 Hz, 1H), 7.02 (d, J = 16.2 Hz, 1H), 6.65 (d, J = 2.1 Hz, 2H), 6.42 (t, J = 2.1 Hz, 1H), 3.81 (s, 6H); ^{13}C NMR (75 MHz, $CDCl_3$) δ 161.0, 141.5, 138.1, 132.4, 132.3, 127.1, 126.8, 118.9, 110.6, 104.9, 100.7, 55.3; CIMS m/z 266 (MH^+); HRMS calcd for $C_{17}H_{15}O_2N$ m/z 265.1103, found: m/z 265.1096 (M^+).

4.2.39. 4-(3,5-Dimethoxyphenethyl)benzenamine (60)

This compound was prepared in 95% yield by following GP 4. Yellow solid: mp 41–42 °C. IR (film) 3368, 2927, 2870, 1597,

1517, 1456, 1105, 967 cm^{-1}; ^1H NMR (300 MHz, $CDCl_3$) δ 7.00 (d, J = 8.1 Hz, 2H), 6.62 (d, J = 8.1 Hz, 2H), 6.36 (d, J = 2.1 Hz, 2H), 6.32 (t, J = 2.1 Hz, 1H), 3.77 (s, 6H), 2.82 (s, 4H); ^{13}C NMR (75 MHz, $CDCl_3$) δ 160.6, 144.4, 144.3, 131.7, 129.1, 115.1, 106.4, 97.8, 55.2, 38.5, 36.8; CIMS m/z 258 (MH^+); HRMS calcd for $C_{16}H_{20}O_2N$ m/z 258.1494, found m/z 258.1495 (MH^+).

4.2.40. 4-(3,4-Dimethoxyphenethyl)aniline (61)

This compound was prepared in 90% yield by following GP 4. Yellow solid: mp 107–108 °C. IR (film) 3363, 2920, 1625, 1515, 1453, 1232, 1144, 1026 cm^{-1}; ^1H NMR (300 MHz, $CDCl_3$) δ 6.96 (d, J = 8.4 Hz, 2H), 6.75 (d, J = 8.1 Hz, 1H), 6.71 (dd, J = 1.8 Hz, 8.4 Hz, 1H), 6.66 (d, J = 1.8 Hz, 1H), 6.63 (d, J = 8.1 Hz, 2H), 3.84 (s, 3H), 3.82 (s, 3H), 3.80 (br, 2H), 2.79 (s, 4H); ^{13}C NMR (75 MHz, $CDCl_3$) δ 148.5, 147.0, 144.2, 134.6, 131.8, 129.2, 120.1, 115.1, 111.7, 111.0, 55.8, 55.7, 37.8, 37.2; CIMS m/z 258 (MH^+); HRMS calcd for $C_{16}H_{19}O_2N$ m/z 257.1416, found: m/z 257.1419 (M^+).

4.2.41. 4-(3,4,5-Trimethoxyphenethyl)aniline (62)[48]

This compound was prepared in 90% yield by following GP 4. Yellow solid: mp 84–85 °C. IR (film) 3368, 1589, 1516, 1457, 1420, 1237, 1124 cm^{-1}; ^1H NMR (300 MHz, $CDCl_3$) δ 6.96 (d, J = 8.4 Hz, 2H), 6.61 (d, J = 8.4 Hz, 2H), 6.36 (s, 2H), 3.82 (s, 6H), 3.81 (s, 3H), 3.50 (br, 2H), 2.79 (s, 4H); ^{13}C NMR (75 MHz, $CDCl_3$) δ 152.9, 144.4, 137.7, 135.9, 131.5, 129.2, 115.1, 105.3, 60.8, 55.9, 38.6, 37.1; ESIMS m/z 288 (MH^+).

4.2.42. 3,4′-(Ethane-1,2-diyl)dibenzenamine (63)

This compound was prepared in 98% yield by following GP 4. White solid: mp 72–73 °C. IR (film) 3390, 3335, 3217, 2915, 1618, 1590, 1515 cm^{-1}; ^1H NMR (300 MHz, $CDCl_3$) δ 7.06 (dd, J = 7.8 Hz, 8.1 Hz, 1H), 6.97 (d, J = 8.1 Hz, 2H), 6.63–6.58 (m, 3H), 6.52–6.50 (m, 2H), 3.42 (br, 4H), 2.77 (s, 4H); ^{13}C NMR (75 MHz, $CDCl_3$) δ 146.2, 144.2, 143.3, 132.0, 129.1, 118.8, 115.2, 115.1, 112.6, 38.2, 36.9; ESIMS m/z 213 (MH^+); HRMS calcd for $C_{14}H_{16}N_2$ m/z 212.1313, found: m/z 212.1314 (M^+).

4.2.43. 3-Amino-4′-amino-*trans*-stilbene (64)

Stannous chloride (435 mg, 2.3 mmol) was added to a solution of (*E*)-4-(3-nitrostyryl)benzenamine (**50**) (110 mg, 0.46 mmol) in ethanol (15 mL), and the reaction mixture was stirred under reflux for 2 h. The ethanol was removed, aq NaOH (1 N, 20 mL) was added to the residue and mixture was stirred for 0.5 h. The aqueous layer was then extracted by diethyl ether (3 × 15 mL) and the organic layer was dried over sodium sulfate. The solvent was evaporated in vacuo at room temperature to provide a yellow solid that was recrystallized from ethyl acetate and hexane to yield a white solid (62 mg, 64.3%): mp 149–150 °C. IR (film) 3392, 3325, 3207, 1598, 1515, 1450, 1291, 970 cm^{-1}; ^1H NMR (300 MHz, $CDCl_3$) δ 7.30 (d, J = 8.4 Hz, 2H), 7.11 (t, J = 7.8 Hz, 1H), 6.96 (d, J = 16.5 Hz, 1H), 6.88 (d, J = 7.8, 1H), 6.81 (d, J = 16.5 Hz, 2H), 6.65 (d, J = 8.4 Hz, 2H), 6.54 (dd, J = 8.4 Hz, 1.8 Hz, 1H), 3.68 (br, 4H); ^{13}C NMR (75 MHz, $CDCl_3$) δ 146.5, 146.0, 129.4, 128.4, 128.0, 127.6, 125.2, 116.9, 115.1, 113.9, 112.5; ESIMS m/z 211 (MH^+); HRMS calcd for $C_{14}H_{14}N_2$ m/z 210.1157, found: m/z 210.1160 (M^+).

4.2.44. 3,5-Diamino-4′-amino-*trans*-stilbene (65)

Stannous chloride (1.08 g, 5.7 mmol) was added to a solution of (*E*)-1,3-dinitro-5-(4-nitrostyryl)benzene (**52**) (100 mg, 0.32 mmol) in ethanol (15 mL) and the reaction mixture was stirred under reflux for 2 h. The ethanol was removed, aq NaOH (1 N, 20 mL) was added to the residue and the mixture was stirred for 0.5 h. The aqueous layer was then extracted by diethyl ether (3 × 15 mL) and the organic layer was dried over sodium sulfate. The solvent was evaporated in vacuo at room temperature to provide a yellow solid that was recrystallized from ethyl acetate and hexane to yield a yellow solid (43.9 mg, 61%): mp 173–174 °C. IR (film) 3338, 1592, 1515, 1462, 965 cm^{-1}; ^1H NMR (300 MHz, $CDCl_3$) δ 7.27 (d, J = 8.4 Hz, 2H), 6.90 (d, J = 16.2 Hz, 1H), 6.72 (d, J = 16.2 Hz, 1H), 6.63 (d, J = 8.4 Hz, 2H), 6.25 (d, J = 1.8 Hz, 2H), 5.93 (t, J = 1.8 Hz, 1H), 3.71 (br, 2H), 3.55 (br, 4H); ^{13}C NMR (75 MHz, $CDCl_3$) δ 147.5, 145.9, 139.9, 128.3, 128.0, 127.6, 125.3, 115.1, 104.0, 101.0; CIMS m/z 226 (MH^+); HRMS calcd for $C_{14}H_{15}N_2$ m/z 255.1266, found: m/z 255.1268 (M^+).

4.2.45. 3,4-Dimethoxy-4′-hydroxyl-*trans*-stilbene (66)[55]

This compound was prepared in 86% yield by following GP 3. Yellow solid: mp 180–181 °C. IR (film) 3369, 2927, 1608, 1516, 1463, 1252, 964 cm^{-1}; ^1H NMR (500 MHz, $CDCl_3$) δ 7.39 (d, J = 8.7 Hz, 2H), 7.05 (d, J = 2.1 Hz, 1H), 7.02 (dd, J = 8.7 Hz, 2.1 Hz, 1H), 6.92 (s, 2H), 6.85 (d, J = 8.7 Hz, 1H), 6.62 (d, J = 8.7 Hz, 2H), 3.94 (s, 3H), 3.90 (s, 3H); ^{13}C NMR (125 MHz, $CDCl_3$) δ 154.9, 148.5, 130.6, 130.4, 127.5, 126.4, 126.2, 119.4, 115.5, 111.1, 108.4, 55.8, 55.7; CIMS m/z 257 (MH^+).

4.2.46. 3,5-Dimethoxy-4′-hydroxyl-*trans*-stilbene (67)[56]

This compound was prepared in 81% yield by following GP 3. White solid: mp 87–88 °C. IR (film) 3368, 1590, 1513, 1455, 1204, 1149, 961 cm^{-1}; ^1H NMR (300 MHz, $CDCl_3$) δ 7.40 (d, J = 8.1 Hz, 2H), 7.03 (d, J = 16.2 Hz, 1H), 6.89 (d, J = 16.2 Hz, 1H), 6.82 (d, J = 8.1 Hz, 2H), 6.65 (d, J = 2.1 Hz, 2H), 6.39 (t, J = 2.1 Hz, 1H), 3.84 (s, 6H); ^{13}C NMR (75 MHz, $CDCl_3$) δ 160.8, 155.3, 139.6, 130.0, 128.6, 127.9, 126.5, 115.5, 104.3, 99.5, 55.3; CIMS m/z 257 (MH^+).

4.2.47. (5-Vinyl-1,3-phenylene)bis(oxy)bis(*tert*-butyldimethylsilane) (69)[57]

Tert-butylchlorodimethylsilane (6.55 g, 43.4 mmol) was added to a well-stirred solution of 3,5-dihydroxybenzaldehyde (**68**) (2 g, 14.48 mmol) and DIPEA (5.56 g, 43.4 mmol) in DMF (20 mL) at 0 °C, and the reaction mixture was stirred for further 3 h at room temperature. The reaction mixture was then diluted with dichloromethane (30 mL), washed with sat aq NaCl (3 × 15 mL) and dried over anhydrous sodium sulfate. The solution was concentrated and the residue was purified by silica gel column chromatography, eluting with a gradient solution from hexane to dichloromethane, to yield 3,5-bis(*tert*-butyldimethylsilyloxy)benzaldehyde as a colorless oil. The solution of 3,5-bis(*tert*-butyldimethylsilyloxy)benzaldehyde in diethyl ether (15 mL) was then added dropwise to a well-stirred solution of methyl triphenylphosphonium bromide (7.1 g, 20 mmol) and sodium amide (780 mg, 20 mmol) in dry diethyl ether (50 mL) at 0 °C. After 10 min, the reaction mixture was warmed up to room temperature and stirred for 2 h. The reaction mixture was filtered and the solvent was removed in vacuo to yield yellow oil that was purified by silica gel column chromatography, eluting with 50% hexane in dichloromethane, to yield a colorless oil (2.7 g, 52%): ^1H NMR (300 MHz, $CDCl_3$) δ 6.61–6.51 (m, 1H), 6.50 (d, J = 2.4 Hz, 2H), 6.23 (t, J = 2.4 Hz, 1H), 5.64 (d, J = 17.7 Hz, 1H), 5.18 (d, J = 10.2 Hz, 1H), 0.95 (s, 18H), 0.18 (s, 12H); ^{13}C NMR (75 MHz, $CDCl_3$) δ 156.5, 139.2, 136.6, 113.8, 111.6, 111.3, 25.6, 18.1, −4.5.

4.2.48. 5-Vinyl-1,3-phenylene diacetate (71)[58]

TBAF (3.41 g, 13.1 mmol) was added dropwise to a solution of (5-vinyl-1,3-phenylene)bis(oxy)bis(*tert*-butyldimethylsilane) (**69**) (2.27 g, 6.22 mmol) in anhydrous THF (15 mL) at 0 °C, and the reaction mixture was then stirred for 3 h at room temperature. The reaction mixture was diluted with diethyl ether (20 mL), washed with sat aq NaCl (3 × 15 mL) and dried over anhydrous sodium sulfate. The solution was concentrated and the residue was purified by silica gel chromatography, eluting with CH_2Cl_2, to yield 5-vinylbenzene-1,3-diol (**70**) (846 mg, 100%) as a colorless oil. Acetic

anhydride (1.83 g, 18 mmol) was added dropwise to a solution of compound **70** (800 mg, 6 mmol), pyridine (1.4 g, 18 mmol) and DMAP (7.32 mg, 0.06 mmol) in CH_2Cl_2 (20 mL) at 0 °C. The reaction mixture was then stirred for 10 h at room temperature and the solution was concentrated to provide a residue that was purified by silica gel column chromatography, eluting with 50% hexane in dichloromethane, to yield **71** (1.17 g, 89%) as a colorless oil: ^{1}H NMR (300 MHz, $CDCl_3$) δ 7.00 (d, J = 2.1 Hz, 2H), 6.80 (t, J = 2.1 Hz, 1H), 6.67–6.58 (m, 4H), 5.71 (d, J = 17.4 Hz, 1H), 5.29 (d, J = 10.2 Hz, 1H), 2.27 (s, 6H); ^{13}C NMR (75 MHz, $CDCl_3$) δ 168.9, 151.1, 139.8, 135.2, 116.7, 115.8, 114.5, 21.0; ESIMS m/z 242 (MNa^+).

4.2.49. 3,5-Diacetoxy-4′-amino-*trans*-stilbene (72)

This compound was prepared in 40% yield by following GP 2. Yellow solid: mp 146–147 °C. IR (film) 3369, 1765, 1601, 1517, 1203, 1122, 964 cm^{-1}; ^{1}H NMR (300 MHz, $CDCl_3$) δ 7.28 (d, J = 8.4 Hz, 2H), 7.05 (d, J = 1.8 Hz, 2H), 6.97 (d, J = 16.5 Hz, 1H), 6.80 (d, J = 16.5 Hz, 1H), 6.74 (t, J = 2.1 Hz, 1H), 6.64 (d, J = 8.4 Hz, 2H), 3.87 (br, 2H), 2.28 (s, 6H); ^{13}C NMR (75 MHz, $CDCl_3$) δ 169.0, 151.1, 146.5, 130.6, 127.9, 127.1, 123.1, 116.3, 115.0, 113.4, 21.1; ESIMS m/z 312 (MH^+); HRMS calcd for $C_{18}H_{18}O_4N$ m/z 312.1236, found: m/z 312.1239 (MH^+).

4.2.50. 3,5-Diacetoxy-4′-nitro-*trans*-stilbene (73)

This compound was prepared in 43% yield by following GP 2. Yellow solid: mp 112–113 °C. IR (film) 3411, 1767, 1593, 1514, 1341, 1198, 1124 cm^{-1}; ^{1}H NMR (300 MHz, $CDCl_3$) δ 8.20 (d, J = 8.7 Hz, 2H), 7. 58 (d, J = 8.7 Hz, 2H), 7.16 (d, J = 16.5 Hz, 1H), 7.15 (d, J = 2.1 Hz, 2H), 7.08 (d, J = 16.5 Hz, 1H), 6.87 (t, J = 2.1 Hz, 1H), 2.30 (s, 6H); ^{13}C NMR (75 MHz, $CDCl_3$) δ 168.9, 151.3, 147.0, 142.9, 138.3, 131.3, 128.1, 127.0, 124.1, 117.3, 115.4, 21.0; CIMS m/z 342 (MH^+); HRMS calcd for $C_{18}H_{15}O_6N$ m/z 341.0899, found: m/z 341.0901 (M^+).

4.2.51. 3,5-Dihydroxyl-4′-amino-*trans*-stilbene (74)

This compound was prepared in 70% yield by following GP 3. Yellow solid: mp 215–216 °C. IR (film) 3368, 1586, 1514, 1473, 1346, 1151, 964 cm^{-1}; ^{1}H NMR (300 MHz, CD_3OD) δ 7.15 (d, J = 8.4 Hz, 2H), 6.80 (d, J = 16.5 Hz, 1H), 6.62 (d, J = 16.5 Hz, 1H), 6.57 (d, J = 8.4 Hz, 2H), 6.31 (d, J = 2.1 Hz, 2H), 6.02 (t, J = 2.1 Hz, 1H); ^{13}C NMR (75 MHz, CD_3OD) δ 159.6, 148.7, 141.6, 129.8, 128.7, 128.6, 125.7, 116.5, 105.6, 102.4; CIMS m/z 228 (MH^+); HRMS calcd for $C_{14}H_{13}O_2N$ m/z 227.0946, found: m/z 227.0944 (M^+).

4.2.52. 3,5-Dihydroxyl-4′-nitro-*trans*-stilbene (75)[59]

This compound was prepared in 81% yield by following GP 3. Yellow solid: mp 256–257 °C. IR (film) 3392, 1600, 1592, 1513, 1334, 1166 cm^{-1}; ^{1}H NMR (300 MHz, CD_3OD) δ 8.20 (d, J = 8.7 Hz, 2H), 7.73 (d, J = 7.5 Hz, 2H), 7.24 (d, J = 16.2 Hz, 1H), 7.13 (d, J = 16.2 Hz, 1H), 6.54 (d, J = 2.1 Hz, 2H), 6.25 (t, J = 2.1 Hz, 1H); ^{13}C NMR (75 MHz, CD_3OD) δ 159.9, 148.0, 145.6, 139.8, 134.8, 128.1, 127.1, 125.0, 106.6, 104.2; CIMS m/z 258 (MH^+).

4.2.53. (3,5-Dimethoxybenzyl)triphenylphosphonium Bromide (78)[60]

$NaBH_4$ (137 mg, 3.61 mmol) was added slowly to a solution of 3,5-dimethoxybenzaldehyde (**5**) (1.5 g, 9.04 mmol) in THF (20 mL). The reaction mixture was stirred for 2 h at room temperature. Water (0.5 mL) was added to the reaction mixture and stirred for 10 min, followed by concentrated HCl (0.29 mL, 3.61 mmol) to neutralize the base. Dichloromethane (25 mL) was added and the organic layer was washed with water (3 × 15 mL) and then dried over anhydrous sodium sulfate. The solvent was removed in vacuo to yield the crude product (3,5-dimethoxyphenyl)methanol (**76**) (1.3 g, 87%). Tribromophosphine (1.6 g, 5.9 mmol) was then added dropwise to a solution of **76** (0.99 g, 5.9 mmol) in dichloromethane (15 mL) at 0 °C. The reaction mixture was stirred for 2 h and then warmed up to room temperature. After 2 h, the organic layer was washed with aq $NaHCO_3$ (3 × 10 mL) and dried over anhydrous sodium sulfate. The solvent was removed in vacuo to yield the crude product 1-(bromomethyl)-3,5-dimethoxybenzene (**77**) (1.65 g, 83.6%), which was then added to a solution of triphenylphosphine (2.1 g, 8 mmol) in anhydrous toluene (20 mL). The resulting mixture was then stirred under reflux for 3 h. The reaction mixture was allowed to cool to room temperature, and the precipitate was filtered and washed with hexane to provide compound **78** (3.5 g, 95%) as white solid: mp 264–265 °C. ^{1}H NMR (300 MHz, $CDCl_3$) δ 7.75–7.66 (m, 9H), 7.62–7.55 (m, 6H), 6.28 (t, J = 2.4 Hz, 2H), 6.24 (t, J = 2.4 Hz, 1H), 5.22 (d, J = 14.4 Hz, 2H), 3.48 (s, 6H); ^{13}C NMR (75 MHz, $CDCl_3$) δ 160.5, 134.9, 134.4, 134.3, 130.1, 129.9, 118.2, 117.0, 109.1, 109.0, 101.2, 55.5.

4.2.54. 2-(1*H*-Imidazol-1-yl)-1-(4-nitrophenyl)ethanone (80)

Imidazole (223 mg, 3.28 mmol) was added to a solution of 2-bromo-1-(4-nitrophenyl)ethanone (**79**) (200 mg, 0.82 mmol) in THF (15 mL) and the reaction mixture was stirred for 15 h at room temperature. THF was then removed in vacuo, and the residue was dissolved in ethyl ether (25 mL). The organic layer was washed with sat aq NaCl (3 × 15 mL) and dried over anhydrous sodium sulfate. The solvent was removed in vacuo to yield a brown solid (140 mg, 90%): mp 164–165 °C. IR (film) 3368, 2921, 1709, 1525, 1347, 1220 cm^{-1}; ^{1}H NMR (300 MHz, $CDCl_3$) δ 8.38 (d, J = 9.0 Hz, 2H), 8.14 (d, J = 9.0 Hz, 2H), 7.54 (s, 1H), 7.15 (s, 1H), 6.95 (s, 1H), 5.50 (s, 2H); ^{13}C NMR (75 MHz, $CDCl_3$) δ 190.3, 150.9, 138.3, 137.9, 129.8, 129.0, 124.2, 120.0, 52.8; CIMS m/z 232 (MH^+); HRMS calcd for $C_{11}H_9O_3N_3$ m/z 231.0644, found: m/z 231.0648 (M^+).

4.2.55. 1-(4-Aminophenyl)-2-(1*H*-imidazol-1-yl)ethanone (81)

Pd/C (10%, 10 mg) was added to a solution of 2-(1*H*-imidazol-1-yl)-1-(4-nitrophenyl)ethanone (**80**) (100 mg, 0.43 mmol) in methanol (20 mL). The suspension was stirred under H_2 for 4 h at 1.5 atm hydrogen pressure. The mixture was filtered, and the solvent was removed in vacuo to provide a yellow solid that was purified by silica gel column chromatography, eluting with 1% methanol in dichloromethane, to yield a yellow solid (69 mg, 79%): mp 201–202 °C. IR (film) 3440, 3427, 3326, 1672, 1655, 1603 cm^{-1}; ^{1}H NMR (300 MHz, CD_3OD) δ 7.80 (d, J = 8.7 Hz, 2H), 7.62 (s, 1H), 7.06 (t, J = 1.2 Hz, 1H), 6.99 (s, 1H), 6.66 (d, J = 8.7 Hz, 2H), 5.52 (s, 2H); ^{13}C NMR (75 MHz, CD_3OD) δ 192.1, 156.1, 139.7, 131.8, 128.4, 123.9, 122.3, 114.3, 52.9; ESIMS m/z 202 (MH^+); HRMS calcd for $C_{11}H_{11}ON_3$ m/z 201.0902, found: m/z 201.0904 (M^+).

4.2.56. (*Z*)-1-(3-(3,5-Dimethoxyphenyl)-2-(4-nitrophenyl)allyl)-1*H*-imidazole (82)

Potassium carbonate (118.7 mg, 0.86 mmol) and a small amount of 18-crown-6 were added to a solution of compounds **80** (100 mg, 0.43 mmol) and **78** (213 g, 0.43 mmol) in anhydrous CH_2Cl_2 (15 mL), the resulting mixture was stirred under reflux for 24 h. The insoluble material was then filtered off and the filtrate was concentrated to provide the orange oil that was purified by flash column chromatography, eluting with a solution of 1% methanol in dichloromethane, to afford **82** (67.5 mg, 43%) as a yellow solid that was recrystallized from hexane and dichloromethane: mp 132–133 °C. IR (film) 3368, 1592, 1515, 1456, 1344, 1204, 1154, 1067, 856 cm^{-1}; ^{1}H NMR (500 MHz, $CDCl_3$) δ 8.18 (d, J = 8.7 Hz, 2H), 7.52 (d, J = 8.7 Hz, 2H), 7.42 (s, 1H), 7.20 (s, 1H), 6.98 (s, 1H), 6.83 (s, 1H), 6.47–6.43 (m, 3H), 5.17 (s, 2H), 3.78 (s, 6H); ^{13}C NMR (125 MHz, $CDCl_3$) δ 161.0, 147.3, 145.9, 137.0, 136.7, 136.5, 134.1, 129.9, 127.1, 124.0, 118.5, 106.4, 100.3, 55.3,

45.8; ESIMS *m/z* 366 (MH^+); HRMS calcd for $C_{20}H_{20}O_4N_3$ *m/z* 366.1454, found: *m/z* 366.1456 (MH^+).

4.2.57. (*Z*)-4-(1-(3,5-Dimethoxyphenyl)-3-(1*H*-imidazol-1-yl) prop-1-en-2-yl)benzenamine (84)

Stannous chloride (259 mg, 1.37 mmol) was added to a solution of (*Z*)-1-(3-(3,5-dimethoxyphenyl)-2-(4-nitrophenyl)allyl)-1*H*-imidazole (**82**) (100 mg, 0.27 mmol) in ethanol (15 mL) and the reaction mixture was stirred under reflux for 2 h. The ethanol was removed, aq NaOH (1 N, 15 mL) was added to the residue and the mixture was stirred for 0.5 h. The aqueous layer was then extracted by diethyl ether (3 × 15 mL) and the organic layer was dried over sodium sulfate. The solvent was evaporated in vacuo at room temperature to provide a yellow solid that was purified by silica gel flash column chromatography, eluting with a solution of 2% methanol in dichloromethane, to provide a white solid (62.5 mg, 69%): mp 134–135 °C. IR (film) 3368, 1590, 1517, 1456, 1204, 1153, 1067, 830 cm^{-1}; ^1H NMR (300 MHz, $CDCl_3$) δ 7.43 (s, 1H), 7.20 (d, *J* = 8.4 Hz, 2H), 7.00 (s, 1H), 6.96 (s, 1H), 6.86 (s, 1H), 6.61 (d, *J* = 8.4 Hz, 2H), 6.40–6.37 (m, 3H), 5.04 (s, 2H), 3.73 (s, 6H), 3.55 (br, 2H); ^{13}C NMR (75 MHz, $CDCl_3$) δ 160.8, 146.6, 138.6, 136.8, 135.0, 130.8, 129.3, 129.1, 127.1, 118.6, 115.0, 106.3, 99.5, 55.2, 46.0; ESIMS *m/z* 336 (MH^+); HRMS calcd for $C_{20}H_{22}O_2N_3$ *m/z* 336.1712, found: *m/z* 336.1714 (MH^+).

4.2.58. 4-Amino-*trans*-stilbene (JH-2-29)[61]

$Pd(OAc)_2$ (51 mg, 0.23 mmol) was added to a well-stirred mixture of compound **85** (0.78 mL, 6.85 mmol) and **24** (1.0 g, 4.57 mmol), Bu_4NBr (2.94 g, 9.13 mmol), and K_2CO_3 (1.58 g, 11.4 mmol) in anhydrous DMF (20 mL) under argon atmosphere at room temperature. The resulting brown solution was stirred at 80 °C under argon atmosphere for 4 h, cooled down to room temperature, and diluted with H_2O (100 mL). 1 M HCl was added to the reaction mixture until pH <5. The resulting suspension was extracted with EtOAc (3 × 100 mL). The combined organic layers were first washed with water (3 × 30 mL) and brine (1 × 30 mL) and dried over sodium sulfate. The solvent was removed under reduced pressure. The crude residue was purified by recrystallization from hexanes to afford **JH-2-29** as a light yellow solid (0.35 g, 40%): mp 148–150 °C. ^1H NMR (300 MHz, acetone-d_6) δ 7.48 (d, *J* = 7.3 Hz, 2H), 7.30–7.28 (m, 2H), 7.17 (tt, *J* = 7.3 Hz, *J* = 1.0 Hz, 1H), 7.09 (d, *J* = 16.2 Hz, 1H), 6.93 (d, *J* = 16.2 Hz, 1H), 6.67 (d, *J* = 8.4 Hz, 2H), 4.82 (s, 2H); ESIMS *m/z* 196 (MH^+).

4.3. Molecular modeling

The crystal structure of aromatase in complex with androgen was downloaded from the Protein Data Bank (PDB code 3eqm).[62] Hydrogens were added and minimized using the Amber force field and the Amber charges. Modeled analogues were constructed in SYBYL 8.1,[63] and energy was minimized with the Amber force field and Amber charges. Docking analogues into the binding site of aromatase was performed using the GOLD program. For the genetic algorithm (GA) runs, a maximum number of 100,000 GA operations were performed on a single population of 100 individuals. Operator weights for crossover, mutation, and migration were set to 95, 95, and 10, respectively, which are the standard default settings recommended by the authors. The maximum distance between hydrogen bond donors and acceptors for hydrogen bonding was set to 3.5 Å. After docking, the best docked conformation of compound **32** was merged into the ligand-free protein. The new ligand–protein complex was subsequently subjected to energy minimization using the Amber force field with Amber charges. During the energy minimization, the structure of the compound **32** and a surrounding 6 Å sphere were allowed to move, while the structures of the remaining protein were frozen. The energy minimization was performed using the Powell method with a 0.05 kcal/(mol Å) energy gradient convergence criterion and a distance-dependent dielectric function.

4.4. Aromatase assay

Aromatase activity was assayed as previously reported, with the necessary modifications to assay in a 384-well plate.[15] Briefly, the test compound (3.5 μL) was preincubated with 30 μL of NADPH regenerating system (2.6 mM $NADP^+$, 7.6 mM glucose 6-phosphate, 0.8 U/mL glucose-6-phosphate dehydrogenase, 13.9 mM $MgCl_2$, and 1 mg/mL albumin in 50 mM potassium phosphate buffer, pH 7.4) for 10 min at 37 °C. The enzyme and substrate mixture (33 μL of 1 μM CYP19 enzyme, BD Biosciences, 0.4 μM dibenzylfluorescein, 4 mg/mL albumin in 50 mM potassium phosphate, pH 7.4) was added, and the plate was incubated for 30 min at 37 °C before quenching with 25 μL of 2 N NaOH. After termination of the reaction and shaking for 5 min, the plate was further incubated for 2 h at 37 °C. This enhances the ratio of signal to background. Fluorescence was measured at 485 nm (excitation) and 530 nm (emission). IC_{50} values were based on three independent experiments performed in duplicate using five concentrations of test substance (Table 1).

Kinetic aromatase assays were carried out in order to determine inhibitor mechanism. Test compound was preincubated with 30 μL of NADPH regenerating system (2.6 mM $NADP^+$, 7.6 mM glucose 6-phosphate, 0.8 U/mL glucose 6-phosphate dehydrogenase, 13.9 mM $MgCl_2$, and 1 mg/mL albumin in 50 mM potassium phosphate buffer, pH 7.4) for 10 min at 37 °C. The IC_{50} was used as the final concentration for each inhibitor. Substrate was added at five concentrations: 16, 8, 4, 2, and 1 μM. CYP19 (1 μM) was added and fluorescence was measured at 485 nm (excitation) and 530 nm (emission) every 10 s for at least 5 min. Error values represent three independent experiments for each compound.

4.5. Expression and purification of human QR2

Human QR2 was purified from 3 L of *Escherichia coli* BL21(DE3) grown in Luria–Bertani medium supplemented with 100 μg/mL ampicillin (Fisher Scientific, Pittsburgh, PA) following our previously reported procedures.[18,24] The concentration of purified QR2 was determined using the Bio-RAD Protein Assay. QR2 was concentrated to 24 mg/mL for crystallization and 4 mg/mL for all kinetics assays. Freshly prepared, non-frozen QR2 was used to set up crystallization experiments. Frozen QR2, previously stored at −80 °C, was thawed on ice and then adjusted to the desired concentration by diluting in storage buffer without glycerol for kinetic assays and inhibitor studies.

4.6. Steady-state kinetic assays and IC_{50} value determination

The catalytic activity of QR2 was determined at 23 °C using a SpectraMax Plus 384 UV–vis microplate reader by monitoring the increase in absorbance at 612 nm, which is due to formation of the product formazan, the reduced form of the substrate MTT [3-(4,5-dimethyltiazol-2-yl)-2,5-diphenyltetrazolium bromide]. Assays were run in 96-well plates with a final assay volume of 200 μL. Each assay mixture contained 12 nM QR2, 17.5 μM NMeH, and 200 μM MTT in a reaction buffer containing 100 mM NaCl, 50 mM Tris, and 0.1% Triton-X100 (Fisher Biotech 93004). All reactions were initiated by the addition of QR2. The initial slopes of the reaction ($\Delta Abs/\Delta time$) were measured and were used to calculate the initial rates of the reaction using a value of 11,300 mM^{-1} cm^{-1} for the molar extinction coefficient.

IC_{50} values, the inhibitory concentration that produces 50% inhibition, were determined in 96-well plates at 23 °C using the

same assay conditions described above except that inhibitor concentrations were varied from 0.2 to 100 μM. Assays at each inhibitor concentration were performed in triplicate, and the average and standard deviations in the rate values were used to determine the final IC_{50} values by calculating the percent inhibition (%I) at each inhibitor concentration versus the negative control with zero inhibitor. The percent inhibition data were then plotted as a function of inhibitor concentration, [I], and the data were then fit to the following equation: $\%I = \%I_{max}/[(1 + [I]/IC_{50})]$ using nonlinear regression describing a simple binding isotherm. All data were globally fit to the equation using the Enzyme Kinetics Module of the program SIGMAPLOT from SPSS Scientific. IC_{50} values are reported along with their standard error in the fitted parameter.

4.7. Crystallization and X-ray structure determination of human QR2 inhibitor complexes

QR2 was crystallized using the hanging-drop, vapor-diffusion method by adding 1 μL of purified QR2 to 1 μL of reservoir solution which contained 1.7 M ammonium sulfate, 0.1 M BisTris, pH 6.5, 0.1 M NaCl, 5 mM DTT, and 12 μM FAD. Diffraction quality crystals grew within two weeks, and individual crystals (approximately 0.1 mm in length) were transferred to a 10 μL solution, prepared with 9 μL of reservoir solution and 1 μL of a stock solution of inhibitor (10 mM in 100% DMSO). The final inhibitor concentration was 0.4 mg/mL and the crystals soaked for 24 h. Crystals were retrieved with a nylon loop which was then used to swipe the crystals through the well solution supplemented with 20% glycerol. The crystals were immediately flash-frozen by plunging into liquid nitrogen. Crystals were stored in shipping dewars containing liquid nitrogen until X-ray data collection.

X-Ray diffraction data were collected at beamline 21-ID-F (λ = 0.978272 Å) at the Life Sciences-Collaborative Access Team (LS-CAT) at the Advanced Photon Source (APS), Argonne National Laboratories. Flash-frozen crystals were transferred from shipping dewars and then mounted on a goniostat under a stream of dry N_2 at 100 K. X-ray data were collected on a MarMosaic 225 mm CCD detector. Complete X-ray data sets were collected on QR2-compound-**32** and QR2-compound-**44** complexes. X-ray data were processed and scaled using the program HKL2000.[64] The structures of both complexes belonged to space group $P2_12_12_1$. Data on the QR2-compound **32** complex were collected to 1.74 Å (1.77–1.74 Å) where the numbers in parentheses represent the highest resolution shell. The overall completeness of the dataset was 91.0% (94.2%) and the average $I/\sigma I$ was 28.5 (4.3). Data on the QR2-compound **44** complex were collected to 1.55 Å (1.58–1.55 Å) resolution with a completeness of 99.7% (99.7%) with an overall average $I/\sigma I$ of 37.2 (5.3).

Intensities were converted to structure-factor amplitudes by the method of French and Wilson[65] using the program TRUNCATE in the CCP4 program suite.[66] The initial phases for the model were determined by the method of molecular replacement using the program PHASER[67] in the CCP4 program suite. The search model used for molecular replacement consisted of the dimer of wild-type QR2 (PDB:2QX4)[24] with all side chains intact and all waters and ligands removed with the exception of FAD. The final and optimal molecular replacement solution contained a single dimer in the asymmetric unit. An initial round of combined positional and B-factor refinement was performed with the program REFMAC[68] in the CCP4 program suite using a maximum-likelihood target function and no sigma cutoff on structure factor amplitudes. Initial difference Fourier maps were calculated and visualized using the program COOT[69] The initial $F_o - F_c$ difference maps revealed strong (+4σ), residual electron density peaks in the active site for the inhibitors. Molecular models for the inhibitors were built using the Monomer Library Sketcher program in the CCP4 program suite, and monomer library descriptions were created for refinement. The inhibitors were manually built into density using the program COOT, and the structures were refined using REFMAC. Iterative rounds of refinement were performed, and water molecules were added manually into strong (+4σ) difference density peaks in the initial refinement stages, and into peaks of (+3σ) in the final stages of refinement. Iterative refinement using REFMAC was continued until the R_{cryst} and R_{free} values reached their lowest plateau values. The final X-ray structural model of the QR2-compound **44** complex was refined to a value of 20.2% (25.6%) for R_{work} and a value of 25.4% (35.2%) for R_{free}. The X-ray structure of the QR2-compound **32** complex was refined to a value of 20.8% (25.5%) for R_{work} and a value of 23.7% (28.6%) for R_{free}. Structural models and electron density maps presented in the figures were produced using the program PYMOL.

Acknowledgments

This work was supported by program project grant P01 CA48112 awarded by the National Cancer Institute. Some of this research was conducted in a facility constructed with the financial support of a Research facilities Improvement program grant C06-14499 from the National Institutes of Health. B.S. wishes to thank China Scholarship Council and Dr. Hongxiang Lou (Shandong University, PR China) for the financial support and assistance. Use of the Advanced Photon Source was supported by the US Department of Energy, Office of Science, Office of Basic Energy Sciences, under Contract No. DE-AC02-06CH11357. Use of the LS-CAT Sector 21 was supported by the Michigan Economic Development Corporation and the Michigan Technology Tri-Corridor research program (Grant 085P1000817).

References and notes

1. Takaoka, M. J. *J. Faculty Sci. Hokkaido Imperial Univ.* **1940**, *3*, 1.
2. Kopp, P. *Eur. J. Endocrinol.* **1998**, *138*, 619.
3. Baur, J. A.; Sinclair, D. A. *Nat. Rev. Drug Disc.* **2006**, *5*, 493.
4. Jemal, A.; Siegel, R.; Ward, E.; Hao, Y.; Xu, J.; Murray, T.; Thun, M. J. *CA Cancer J. Clin.* **2008**, *58*, 71.
5. Chen, S.; Zhou, D.; Okubo, T.; Kao, Y. C.; Eng, E. T.; Grube, B.; Kwon, A.; Yang, C.; Yu, B. *Ann. N.Y. Acad. Sci.* **2002**, *963*, 229.
6. Brueggemeier, R. W.; Richards, J. A.; Joomprabutra, S.; Bhat, A. S.; Whetstone, J. L. *J. Steroid Biochem. Mol. Biol.* **2001**, *79*, 75.
7. Banting, L.; Nicholls, P. J.; Shaw, M. A.; Smith, H. J. *Prog. Med. Chem.* **1989**, *26*, 253.
8. Lonard, D. M.; Smith, C. L. *Steroids* **2002**, *67*, 15.
9. Park, W. C.; Jordan, V. C. *Trends Mol. Med.* **2002**, *8*, 82.
10. Nicholls, H. *Trends Mol. Med.* **2002**, *8*, S12–S13.
11. Miller, W. R. *Best. Pract. Res. Clin. Endocrinol. Metab.* **2004**, *18*, 1.
12. Miller, W. R. *Semin. Oncol.* **2003**, *30*, 3.
13. Buzdar, A. U. *Clin. Breast Cancer* **2003**, *4*, S84.
14. Recanatini, M.; Cavalli, A.; Valenti, P. *Med. Res. Rev.* **2002**, *22*, 282.
15. Maiti, A.; Cuendet, M.; Croy, V. L.; Endringer, D. C.; Pezzuto, J. M.; Cushman, M. *J. Med. Chem.* **2007**, *50*, 2799.
16. Mokbel, K. *Int. J. Clin. Oncol.* **2002**, *7*, 279.
17. Wang, Y.; Lee, K. W.; Chan, F. L.; Chen, S.; Leung, L. K. *Toxicol. Sci.* **2006**, *92*, 71.
18. Maiti, A.; Reddy, P. V. N.; Sturdy, M.; Marler, L.; Pegan, S. D.; Mescar, A. D.; Pezzuto, J. M.; Cushman, M. *J. Med. Chem.* **2009**, *52*, 1873.
19. Celli, C. M.; Tran, N.; Knox, R.; Jaiswal, A. K. *Biochem. Pharmacol.* **2006**, *72*, 366.
20. Jamieson, D.; Tung, A. T.; Knox, R. J.; Boddy, A. V. *J. Cancer.* **2006**, *95*, 1229.
21. Knox, R. J.; Jenkins, T. C.; Hobbs, S. M.; Chen, S.; Melton, R. G.; Burke, P. J. *Cancer Res.* **2000**, *60*, 4179.
22. Buryanovskyy, L.; Fu, Y.; Boyd, M.; Ma, Y. L.; Hsieh, T. C.; Wu, J. M.; Zhang, Z. T. *Biochemistry* **2004**, *43*, 11417.
23. Boutin, J. A.; Audinot, V.; Ferry, G.; Delagrange, P. *Trends Pharmacol. Sci.* **2005**, *26*, 412.
24. Calamini, B.; Santarsiero, B. D.; Boutin, J. A.; Mesecar, A. D. *Biochem. J.* **2008**, *413*, 81.
25. Angela, F.; Carolina, F.; Carolina, M.; Marcella, G.; Giulia, N. *Nat. Prod. Res., Part A* **2007**, *21*, 564.
26. Sun, B.; Yuan, H. Q.; Xi, G. M.; Ma, Y. D.; Lou, H. X. *Bioorg. Med. Chem.* **2009**, *17*, 4981.
27. Eicher, T.; Fey, S.; Puhl, W.; Büchel, E.; Speicher, A. *Eur. J. Org. Chem.* **1998**, *5*, 877.
28. Ghosh, D.; Griswold, J.; Erman, M.; Pangborn, W. *Nature* **2009**, *457*, 219.

29. Verdonk, M. L.; Cole, J. C.; Hartshorn, M. J.; Murray, C. W.; Taylor, R. D. *Proteins* **2003**, *52*, 609.
30. Jones, G.; Willett, P.; Glen, R. C.; Leach, A. R.; Taylor, R. *J. Mol. Biol.* **1997**, *267*, 727.
31. Wang, R.; Lu, Y.; Wang, S. *J. Med. Chem.* **2003**, *46*, 2287.
32. Recanatini, M.; Bisi, A.; Cavalli, A.; Belluti, F.; Gobbi, S.; Rampa, A.; Valenti, P.; Palzer, M.; Palusczak, A.; Hartmann, R. F. *J. Med. Chem.* **2001**, *44*, 672.
33. Leonetti, F.; Favia, A.; Rao, A.; Aliano, R.; Paluszcak, A.; Hartmann, R. F.; Carotti, A. *J. Med. Chem.* **2004**, *47*, 6792.
34. Gobbi, S.; Cavalli, A.; Negri, M.; Schewe, K. E.; Belluti, F.; Piazzi, L.; Hartmann, R. W.; Recanatini, M.; Bisi, A. *J. Med. Chem.* **2007**, *50*, 3420.
35. Neves, M. A. C.; Dinis, T. C. P.; Colombo, G.; Melo, M. L. S. *J. Med. Chem.* **2009**, *52*, 143.
36. Saberi, M. R.; Vinh, T. K.; Yee, S. W.; Griffiths, N.; Evans, P. J.; Simons, C. *J. Med. Chem.* **2006**, *49*, 1016.
37. Carreno, M. C.; Mahugo, J.; Urbano, A. *Tetrahedron Lett.* **1997**, *38*, 3047.
38. Takashima, Y.; Kaneko, Y.; Kobayashi, Y. *Tetrahedron* **2010**, *66*, 197.
39. Marx, V. M.; Burnell, D. J. *J. Am. Chem. Soc.* **2010**, *132*, 1685.
40. Alonso, F.; Riente, P.; Yus, M. *Eur. J. Org. Chem.* **2009**, *34*, 6034.
41. Arrish, J. P.; Jung, Y. C.; Shin, S.; Jung, K. W. *J. Org. Chem.* **2002**, *67*, 7127.
42. Waterman, P. G. *Phytochemistry* **1976**, *15*, 347.
43. Banerjee, B.; Capps, S. G.; Kang, J.; Robinson, J. W.; Castle, S. L. *J. Org. Chem.* **2008**, *73*, 8973.
44. Marcoux, D.; Goudreau, S. R.; Charette, A. B. *J. Org. Chem.* **2009**, *74*, 8939.
45. Coe, B. J.; Hamor, T. A.; Jones, C. J.; McCleverty, J. A.; Bloor, D.; Cross, G. H.; Axon, T. L. *J. Chem. Soc., Dalton. Trans.* **1995**, *4*, 673.
46. Motoshima, K.; Noguchi-Yachide, T.; Sugita, K.; Hashimoto, Y.; Ishikawa, M. *Bioorg. Med. Chem.* **2009**, *17*, 5001.
47. Velder, J.; Ritter, S.; Lex, J.; Schmalz, H. G. *Synthesis* **2006**, *2*, 273.
48. Cushman, M.; Nagarathnam, D.; Gopal, D.; Chakraborti, A. K.; Lin, C. M.; Hamel, E. *J. Med. Chem.* **1991**, *34*, 2579.
49. Ling, C.; Minato, M.; Lahti, P. M.; Van Willigen, H. *J. Am. Chem. Soc.* **1992**, *114*, 9959.
50. Iding, H.; Jolidon, S.; Krummenacher, D.; Rodriguez, S. R. M.; Thomas, A. W.; Wirz, B.; Wostl, W.; Wyler, R. *PCT Int. Appl.* **2004**, 55.
51. Liu, H.; Dong, A.; Gao, C.; Tan, C.; Liu, H.; Zu, X.; Jiang, Y. *Bioorg. Med. Chem.* **2008**, *16*, 10013.
52. Moro, A. V.; Cardoso, F. S. P.; Correia, C. R. D. *Tetrahedron Lett.* **2008**, *49*, 5668.
53. Moran, B. W.; Anderson, F. P.; Devery, A.; Cloonan, S.; Butler, W. E.; Varughese, S.; Draper, S. M.; Kenny, P. T. M. *Bioorg. Med. Chem.* **2009**, *17*, 4510.
54. Mizuno, C. S.; Schrader, K. K.; Rimando, A. M. *J. Agric. Food Chem.* **2008**, *56*, 9140.
55. Kang, S. S.; Cuendet, M.; Endringer, D. C.; Croy, V. L.; Pezzuto, J. M.; Lipton, M. A. *Bioorg. Med. Chem.* **2009**, *17*, 1044.
56. Suresh, A.; Tatsuya, M.; Zaw, L. T.; Feng, L.; Nwet, W.; Yasuhiro, T.; Hiroyasu, E.; Shigetoshi, K. *J. Nat. Prod.* **2009**, *72*, 1631.
57. Angela, F.; Carolina, F.; Carolina, M. *Nat. Prod. Res. Part A: Struct. Synth.* **2006**, *20*, 247.
58. Marcella, G.; Carolina, M.; Angela, F. *Tetrahedron Lett.* **2002**, *43*, 597.
59. Michael, M.; Jill, M.; Johan, A.; Carmen, A.; Marie, L.; Michelle, D. *PCT Int. Appl.* **2007**, 337.
60. Gabriele, B.; Benabdelkamel, H.; Plastina, P.; Fazio, A.; Sindona, G.; Donna, L. D. *Synthesis* **2008**, *18*, 2953.
61. Arvela, R. K.; Leadbeater, N. E.; Sangi, M. S.; Williams, V. A.; Granados, P.; Singer, R. D. *J. Org. Chem.* **2005**, *70*, 161.
62. www.rcsb.org.
63. SYBYL 8.1 for Linux; Tripos, Inc.: 2007. 1699 South Hanley Rd., St. Louis, MO 63144-2917, USA.
64. Otwinowski, Z.; Minor, W. Processing of X-ray Diffraction Data Collected in Oscillation Mode. In *Methods in Enzymology, Part A*; Carter, C. W., Jr., Sweet, R. M., Eds.; Academic Press: New York, 1997; Vol. 276, p 307.
65. French, S.; Wilson, K. *Acta Cryst.* **1994**, *A34*, 517.
66. CCP4, Collaborative Project Number 4, *Acta Cryst.* **1994**, *D50*, 760.
67. Storoni, L. C.; McCoy, A. J.; Read, R. J. *Acta Crystallogr., Sect D* **2004**, *60*, 432.
68. Murshudov, G. N.; Vagin, A. A.; Dodson, E. J. *Acta Crystallogr., Sect D* **1997**, *53*, 240.
69. Emsley, P.; Cowtan, K. *Acta Crystallogr., Sect D* **2004**, *60*, 2126.